IEEE Access
Multidisciplinary | Rapid Review | Open Access Journal

Received May 19, 2021, accepted May 27, 2021, date of publication June 2, 2021, date of current version June 9, 2021.

Digital Object Identifier 10.1109/ACCESS.2021.3085349

One-Sided and Two One-Sided Multivariate Homogeneously Weighted Moving Charts for Monitoring Process Mean

NURUDEEN A. ADEGOKE[1], MUHAMMAD RIAZ[2], KHADIJAT OLADAYO GANIYU[3], AND SADDAM AKBER ABBASI[4]

[1]School of Natural and Computational Sciences, Massey University, Albany, Auckland 0632, New Zealand
[2]Department of Mathematics and Statistics, King Fahd University of Petroleum and Minerals, Dhahran 31261, Saudi Arabia
[3]AsureQuality Laboratory, Auckland 1060, New Zealand
[4]Department of Mathematics, Statistics and Physics, Qatar University, Doha, Qatar

Corresponding author: Muhammad Riaz (riazm@kfupm.edu.sa)

This work was supported by the Deanship of Scientific Research (DSR) at King Fahd University of Petroleum and Minerals (KFUPM) under Grant SB191043.

ABSTRACT Multivariate memory-type control charts that use information from both the current and previous process observations have been proposed. They are designed to detect shifts in both upper and downward directions with equal precision when monitoring the process mean vector. The absence of directional sensitivity can limit the charts' application, particularly when users are interested in detecting variations in one direction than the other. This article proposes one-sided and two one-sided multivariate control charts for monitoring shifts in the process mean vector. The proposed charts are presented in the form of the multivariate homogeneously weighted moving average approach that yields efficient detection of shifts in the mean vector. We provide simulation studies under different shift sizes in the process mean vector and evaluate the performance of the proposed charts in terms of their run length properties. We compare the average run length (ARL) results of the charts with the conventional charts as well as the one-sided and two one-sided multivariate exponentially weighted moving average (MEWMA) and multivariate cumulative sum (MCUSUM) charts. Our simulation results show that the proposed charts outperform the existing charts used for the same purpose, particularly when interest lies in detecting small shifts in the mean vector. We show how the charts can be designed to be robust to non-normal distributions and give a step-by-step implementation efficient application of the charts when their parameters are unknown and need to be estimated. Finally, an illustrative example is provided to show the application of the proposed charts.

INDEX TERMS Average run length, multivariate homogeneously weighted moving average, one-sided control charts, two one-sided control charts, robustness, estimation.

I. INTRODUCTION

Multivariate process control (MPC) is used to monitor processes comprising several correlated characteristics or features. Several MPC tools, which are multivariate extensions of univariate charts for monitoring single process characteristic, have been proposed in practice. They are useful in ensuring that any changes in the process are detected early to avoid several anomalies on the final products. The first MPC tool can be traced back to work by [1], who developed the χ^2 chart. It is a multivariate analogue of the univariate Shewhart chart [2]. The chart gives a signal of mean shift whenever the chart's statistic is greater than $\chi^2_{(p,\alpha)}$, where $\chi^2_{(p,\alpha)}$ is the α^{th} upper percentage point of the chi-square distribution with the p degrees of freedom.

The χ^2 chart is useful for detecting large shifts in the mean vector but less sensitive in detecting small to moderate shifts in the process characteristics. To enhance the sensitivity of the χ^2 chart to detect small shifts in the process mean vector, different multivariate memory-type tools that use information from both the current and previous process observations have also been proposed in the literature. For example, [3] and [4]

The associate editor coordinating the review of this manuscript and approving it for publication was Paolo Giangrande.

proposed multivariate cumulative sum (CUSUM) control charts which are the multivariate extensions of the univariate CUSUM chart proposed by [5]. [6] proposed the multivariate exponentially weighted moving average (EWMA) control chart, which is a multivariate extension of the univariate EWMA chart by [7]. Also, [8] proposed the multivariate homogeneously weighted moving average (MHWMA) control chart, which is a multivariate extension of the univariate HWMA chart by [9]. Average run length (ARL) comparison of the MHWMA chart with the competing charts, including the chi-square chart, the MEWMA chart and the MCUSUM chart, showed that the MHWMA chart outperformed the other charts when interest lies in detecting small shifts in the process mean vector.

Different enhancement of the MEWMA, MCUSUM and MHWMA charts have been proposed in practice. For example, [4] studied the zero-state and steady-state average length (ARL) performance of the MEWMA chart. [10] proposed optimal statistical design for multivariate CUSUM (MCUSUM) chart. [11] integrated conforming run-length chart with MCUSUM to propose a synthetic MCUSUM chart. [12], [13] improved the sensitivity of MCUSUM and MEWMA charts using shrinkage estimates of the covariance matrix. [14] compared the performance of the MEWMA, MCUSUM and MHWMA charts when the charts' parameters are estimated. [15]–[17] proposed adaptive versions of MCUSUM and MEWMA charts for the process mean based on fixed and variable sampling intervals. We refer interested to [18]–[22] for some recent enhancements of the MEWMA, MCUSUM and MHWMA charts.

The multivariate charts and their enhancements mentioned above are directional invariant charts. They are proposed to detect shifts in all directions (i.e., upper and downward) with equal precision when monitoring the process mean vector. The absence of directional sensitivity can limit the charts' application, particularly when users are interested in detecting variations or changes in some directions more than others. Such directional charts could allow practitioners to detect an increase or a decrease in quality characteristics. For example, the use of the directional invariant chart or its modifications may fail or ineffective to detect or give prompt warnings of bioterrorist attacks or other arising health conditions, such as high-level toxicity of drugs, increase or decrease in naturally occurring disease outbreak or an increased health risk to the public [23]–[25]. Specifically, directional invariant charts may take a much longer time to detect signals when the signals are far below the target than if they were close to the target when the shift occurred. On the other hand, using a one-sided chart can improve the speed in detecting an upward or a downward change in the process mean vector.

To this end, [24] proposed a one-sided MCUSUM chart. The one-sided MCUSUM due to [24] outperforms the MCUSUM chart of [3] when detecting either upward or downward shifts in the process mean vector. [23] proposed a one-sided MEWMA chart for monitoring process mean vector. Recently, a directionally more sensitive one-sided MEWMA chart was proposed by [26]. The one-sided MEWMA chart due to [26] used a transformation that truncates observations that is either above and below the process mean vector. Also, [25] proposed a one-sided MCUSUM chart for monitoring the mean vector of a multivariate normal process. However, unlike the one-sided MEWMA and MCUSUM charts, one-sided MHWMA charts have received no attention in SPC literature to the best of our knowledge.

Hence, two different one-sided MHWMA-based charts that assume a known upward or downward shift are proposed in this manuscript. The charts accumulate positive (or negative) deviations from the target. The first one-sided upper chart (hereafter referred to as the OMHWMAI chart) accumulates observations above the target and truncates observations below the target to the target value. The second upper one-sided chart (hereafter referred to as the OMHWMAII chart), on the other hand, accumulates observations above the observed MHWMA statistic value and truncates observations below the value to the target value. We also provide two one-sided versions of the one-sided charts that can be used to detect irregular changes (i.e., both upward and downward shifts) in the process mean vector.

A brief introduction of the classical MHWMA chart and the designs of the proposed one-sided and two one-sided charts are discussed in Section II. The performance evaluation of the charts and their comparison with existing one-sided and two one-sided charts in literature are provided in Section III. The sensitivity of the charts to non-normality is studied in Section IV. We provide a step-by-step implementation of the charts when their parameters are unknown in Section V. An illustrative example of the proposed charts for monitoring aquatic toxicity level is given in Section VI. Lastly, conclusions and directions for future work are presented in Section VII.

II. THE PROPOSED ONE-SIDED AND TWO ONE-SIDED MHWMA CHARTS

A. BRIEF SUMMARY OF THE CLASSICAL MHWMA CHART

Suppose $p \times n$ independently and identically distributed multivariate normal random variables $\boldsymbol{Y_1}, \boldsymbol{Y_2}, \ldots$, with mean vector $\boldsymbol{\mu}$ and covariance matrix $\boldsymbol{\Sigma}$ are available for monitoring. We assume the in-control values of the parameters $\boldsymbol{\mu}$ and $\boldsymbol{\Sigma}$ for the normal operating process are $\boldsymbol{\mu}_0$ and $\boldsymbol{\Sigma}_0$, respectively. Also, we assume the values of $\boldsymbol{\mu}_0$ and $\boldsymbol{\Sigma}_0$ are known apriori or there are well-defined Phase I in-control sample from which they can be estimated. We standardized the random variable $\boldsymbol{Y}_i$ to obtain $\boldsymbol{X}_i$ given as $\boldsymbol{X}_i = \boldsymbol{\Sigma}_0^{-1/2}(\boldsymbol{Y}_i - \boldsymbol{\mu}_0)$, such that in general $\boldsymbol{X}$ is distributed as $N(\boldsymbol{\mu}_*, \boldsymbol{\Sigma}_*)$, where $\boldsymbol{\mu}_* = \boldsymbol{\Sigma}_0^{-\frac{1}{2}}(\boldsymbol{\mu} - \boldsymbol{\mu}_0)$ and $\boldsymbol{\Sigma}_* = \boldsymbol{\Sigma}_0^{-\frac{1}{2}}\boldsymbol{\Sigma}\boldsymbol{\Sigma}_0^{-\frac{1}{2}}$. When the process is in control, the transformed variable $\boldsymbol{X}$ is distributed as a standard normal distribution(i.e., $N(\boldsymbol{0}, \boldsymbol{I}_p)$), where $\boldsymbol{I}_p$ is a $p \times p$ identity matrix.

The monitoring statistic of the MHWMA chart for monitoring the mean vector of an individual-observation is defined

as

$$\boldsymbol{H_i} = w\boldsymbol{x_i} + (1-w)\boldsymbol{x}_{i-1}^{-}, \tag{1}$$

where $i = 1, 2, \ldots,$. $\bar{\boldsymbol{x}}_{i-1}$ represents the sample average of the previous information up to and including the $i-1$ observation, and $\bar{\boldsymbol{x}}_0 = \mathbf{0}$. The smoothing parameter w is selected such that $0 < w \leq 1$. The mean vector and covariance of the statistic $\boldsymbol{H}_i$ are given as $\boldsymbol{\mu}_H = \mathbf{0}$ and

$$\boldsymbol{\Sigma}_{\boldsymbol{H}_i} = \begin{cases} w^2\boldsymbol{I}_p & \text{if } i = 1 \\ w^2\boldsymbol{I}_p + (1-w)^2\dfrac{\boldsymbol{I}_p}{i-1} & \text{if } i > 1, \end{cases} \tag{2}$$

respectively [8]. The MHWMA chart gives an out-of-control signal whenever $T_i^2 = \boldsymbol{H_i}'\boldsymbol{\Sigma_{Hi}}^{-1}\boldsymbol{H_i} > h$. The parameters h and w are chosen to achieve a desired in-control performance measure of the chart, such as the desired in-control ARL performance, and $\boldsymbol{\Sigma_{Hi}}$ is the covariance matrix of $\boldsymbol{H}$ at time point i. The MHWMA chart is a directionally invariant chart; the ARL performance of the chart depends on $\boldsymbol{\mu_0}$ and $\boldsymbol{\Sigma_0}$, only through the non-centrality parameter given as $\boldsymbol{\delta} = \left(\boldsymbol{\mu_1'}\boldsymbol{\Sigma_0^{-1}}\boldsymbol{\mu_1}\right)^{1/2}$, where $\boldsymbol{\mu_1}$ is the mean vector for the out-of-control process.

B. THE PROPOSED ONE-SIDED AND TWO ONE-SIDED MHWMA CHARTS

1) ONE-SIDED MHWMA CHARTS

Two different one-sided upper MHWMA-based charts, referred to as OMHWMAI and OMWMAII charts, that assume upward shifts in the mean vector are provided in this section. The OMHWMAI chart is obtained by transforming the vector of observation $\boldsymbol{X}_i$ into $\boldsymbol{X}_i^+$, given as $\boldsymbol{X}_i^+ = +\max(\mathbf{0}, \boldsymbol{X_i})$, and then define MHWMA structure based on $\boldsymbol{X}_i^+$, where $+\max\{.\}$ returns the (parallel) maxima of the input vectors. The vector $\boldsymbol{X}_i^+$ accumulates observations that are above the zero vector and truncated the observations that are less than the $\boldsymbol{X}_i$ to zero vector. When the process is in control, the mean vector and covariance matrix of the transformed variable $\boldsymbol{X}_i^+$ are given by

$$\boldsymbol{\mu}_{\boldsymbol{X}_i^+} = \frac{1}{\sqrt{2\pi}} \times \mathbf{1}_p \tag{3}$$

and

$$\boldsymbol{\Sigma}_{\boldsymbol{X}_i^+} = \left(\frac{1}{2} - \frac{1}{2\pi}\right)^{1/2} \boldsymbol{I}_{p\times p}, \tag{4}$$

respectively, where $\mathbf{1}_p$ is a column vector. Let $\boldsymbol{I}_i^+$ be the MHWMA sequence based on $\boldsymbol{X}_i^+$, given by

$$\boldsymbol{I}_i^+ = w(\boldsymbol{X}_i^+ - \boldsymbol{\mu}_{\boldsymbol{X}_i^+}) + (1-w)\bar{\boldsymbol{X}}_{i-1}^+, \tag{5}$$

where $\bar{\boldsymbol{X}}_0^+ = \mathbf{0}$. The OMHWMAI chart involves plotting $T_i^2 = \boldsymbol{I}_i^{+\prime}\boldsymbol{\Sigma}_{\boldsymbol{I}_i^+}^{-1}\boldsymbol{I}_i^+$, where

$$\boldsymbol{\Sigma}_{\boldsymbol{I}_i^+} = \begin{cases} w^2\boldsymbol{\Sigma}_{\boldsymbol{X}_i^+} & \text{if } i = 1 \\ w^2\boldsymbol{\Sigma}_{\boldsymbol{X}_i^+} + (1-w)^2\dfrac{\boldsymbol{\Sigma}_{\boldsymbol{X}_i^+}}{i-1} & \text{if } i > 1 \end{cases} \tag{6}$$

The chart detects out-of-control upper signal whenever $T_i^2 = \boldsymbol{I}_i^{+\prime}\boldsymbol{\Sigma}_{\boldsymbol{I}_i^+}^{-1}\boldsymbol{I}_i^+ > h$.

The OMHWMAII chart on the other hand uses the transformation $\boldsymbol{Z}_i^+ = +\max(\mathbf{0}, \boldsymbol{H_i})$, where the vector $\boldsymbol{H_i}$ is given in equation (1). The statistic $\boldsymbol{Z}_i^+$ accumulates observations that are above the $\mathbf{0}$ and truncated the observations that are less than the $\boldsymbol{H_i}$ to the zero vector. When the process is in control, we approximate the mean vector and covariance matrix of the transformed variable $\boldsymbol{Z}_i^+$ by

$$\boldsymbol{\mu}_{\boldsymbol{Z}_i^+} = \begin{cases} \dfrac{1}{\sqrt{2\pi}} w \times \mathbf{1}_p & \text{if } i = 1 \\ \dfrac{1}{\sqrt{2\pi}}\sqrt{(w^2 + (1-w)^2\dfrac{1}{i-1})} \times \mathbf{1}_p & \text{if } i > 1 \end{cases} \tag{7}$$

and

$$\boldsymbol{\Sigma}_{\boldsymbol{Z}_i^+} = \begin{cases} w^2\boldsymbol{\Sigma}_{\boldsymbol{X}_i^+} & \text{if } i = 1 \\ w^2\boldsymbol{\Sigma}_{\boldsymbol{X}_i^+} + (1-w)^2\dfrac{\boldsymbol{\Sigma}_{\boldsymbol{X}_i^+}}{i-1} & \text{if } i > 1 \end{cases} \tag{8}$$

respectively. The OMHWMAII chart detects out-of-control upper signal whenever $T_i^2 = (\boldsymbol{Z}_i^+ - \boldsymbol{\mu}_{\boldsymbol{Z}_i^+})'\boldsymbol{\Sigma}_{\boldsymbol{Z}_i^+}^{-1}(\boldsymbol{Z}_i^+ - \boldsymbol{\mu}_{\boldsymbol{Z}_i^+}) > h$. The smoothing parameters w of the OMHWMAI and OMHWMAII charts are selected such that $0 < w \leq 1$. The values of h and w of the charts are chosen to achieve a desired in-control ARL.

2) THE PROPOSED TWO ONE-SIDED MHWMA CHARTS

In order to devise MHWMA charts that can detect both increases and decreases in the process mean vector, we integrate two one-sided MHWMA charts for detecting upper and lower mean shifts into a single chart. We consider two multivariate normal vectors that can take either positive or negative values. The MHWMA charting procedure is then applied to these vectors to obtain the two one-sided MHWMA charts for detecting increase and decrease shifts in the process mean vector. Here, we provide two one-sided MHWMA charts, referred to as TMHWMAI and TMWMAII charts, for monitoring increasing and decreasing changes in the process mean vector. The TMHWMAI and TMWMAII charts are two one-sided versions of the OMHWMAI and OMWMAII charts, respectively.

Similar to the OMHWMAI chart, the TMHWMAI chart is obtained by first transforming the observation $\boldsymbol{X}_i$ into $\boldsymbol{X}_i^+ = +\max(\mathbf{0}, \boldsymbol{X_i})$ and $\boldsymbol{X}_i^- = -\min(\mathbf{0}, \boldsymbol{X_i})$, respectively, and then define MHWMA structure based on $\boldsymbol{X}_i^+$ and $\boldsymbol{X}_i^-$, where $+\max\{.\}$ and $-\min\{.\}$ return the (parallel) maxima and minima of the input vectors, respectively. The vector $\boldsymbol{X}_i^+$ accumulates observations that are above the zero and truncated the observations that are less than the $\boldsymbol{X}_i$ to zero vector. In contrast, $\boldsymbol{X}_i^-$ accumulates observations that are below the zero and truncated the observations that are greater than $\boldsymbol{X}_i$ to the zero vector. When the process is in control, the mean vector and covariance matrix of the transformed variable $\boldsymbol{X}_i^+$ are $\boldsymbol{\mu}_{\boldsymbol{X}_i^+}$ (given in equation 3) and $\boldsymbol{\Sigma}_{\boldsymbol{X}_i^+}$ (given in equation 4), respectively. Also, the mean vector and covariance matrix of

the transformed variable $\boldsymbol{X}_i^-$ are $\boldsymbol{\mu}_{\boldsymbol{X}_i^-} = -\boldsymbol{\mu}_{\boldsymbol{X}_i^+}$ and $\boldsymbol{\Sigma}_{\boldsymbol{X}_i^-} = \boldsymbol{\Sigma}_{\boldsymbol{X}_i^+}$, respectively. Let $\boldsymbol{I}_i^+$ and $\boldsymbol{I}_i^-$ be the two MHWMA sequences based on $\boldsymbol{X}_i^+$ and $\boldsymbol{X}_i^-$, respectively, given by

$$\boldsymbol{I}_i^+ = w(\boldsymbol{X}_i^+ - \boldsymbol{\mu}_{\boldsymbol{X}_i^+}) + (1-w)\bar{\boldsymbol{X}}_{i-1}^+ \tag{9}$$

$$\boldsymbol{I}_i^- = w(\boldsymbol{X}_i^- - \boldsymbol{\mu}_{\boldsymbol{X}_i^-}) + (1-w)\bar{\boldsymbol{X}}_{i-1}^- \tag{10}$$

where $\bar{\boldsymbol{X}}_0^+ = \bar{\boldsymbol{X}}_0^- = \boldsymbol{0}$. The TMHWMAI chart detects out-of-control upper or lower signals whenever $\boldsymbol{I}_i{}^{+\prime}\boldsymbol{\Sigma}_{\boldsymbol{I}_i^+}^{-1}\boldsymbol{I}_i^+ > h$ or $\boldsymbol{I}_i^{-\prime}\boldsymbol{\Sigma}_{\boldsymbol{I}_i^-}^{-1}\boldsymbol{I}_i^- > h$, respectively, where $\boldsymbol{\Sigma}_{\boldsymbol{I}_i^+}$ is given in equation (6).

The TMHWMAII chart (the two one sided version of the OMWMAII chart) is obtained by transforming $\boldsymbol{H_i}$ (in equation (1)) into $\boldsymbol{Z}_i^+ = +\max(\boldsymbol{0}, \boldsymbol{H_i})$ and $\boldsymbol{Z}_i^- = -\min(\boldsymbol{0}, \boldsymbol{H_i})$. The statistic $\boldsymbol{Z}_i^+$ accumulates observations that are above the $\boldsymbol{0}$ and truncated the observations that are less than $\boldsymbol{H_i}$ to the zero vector. On the other hand, the statistic $\boldsymbol{Z}_i^-$ accumulates observations that are below the $\boldsymbol{0}$, and truncated the observations that are greater than $\boldsymbol{H_i}$ to zero vector. When the process is in control, the mean vector and covariance matrix of the transformed variable $\boldsymbol{Z}_i^+$ are $\boldsymbol{\mu}_{\boldsymbol{Z}_i^+}$ (given in equation 7) and $\boldsymbol{\Sigma}_{\boldsymbol{Z}_i^+}$ (given in equation 8), respectively. Also, the mean vector and covariance matrix of the transformed variable $\boldsymbol{Z}_i^-$ are $\boldsymbol{\mu}_{\boldsymbol{Z}_i^-} = -\boldsymbol{\mu}_{\boldsymbol{Z}_i^+}$ and $\boldsymbol{\Sigma}_{\boldsymbol{Z}_i^-} = \boldsymbol{\Sigma}_{\boldsymbol{Z}_i^+}$, respectively. The TMHWMAII chart detects out-of-control upper or lower signals whenever $(\boldsymbol{Z}_i^+ - \boldsymbol{\mu}_{\boldsymbol{Z}_i^+})'\boldsymbol{\Sigma}_{\boldsymbol{Z}_i^+}^{-1}(\boldsymbol{Z}_i^+ - \boldsymbol{\mu}_{\boldsymbol{Z}_i^+}) > h$ or $(\boldsymbol{Z}_i^- - \boldsymbol{\mu}_{\boldsymbol{Z}_i^-})'\boldsymbol{\Sigma}_{\boldsymbol{Z}_i^-}^{-1}(\boldsymbol{Z}_i^- - \boldsymbol{\mu}_{\boldsymbol{Z}_i^-}) > h$, respectively. The smoothing parameters of the TMHWMAI and TMHWMAII charts w are selected such that $0 < w \leq 1$. Also, the values of h and w for the charts are chosen to achieve a desired in-control ARL.

III. PERFORMANCE EVALUATION AND COMPARISON

In this section, we study the zero-state and steady-state run-length performance of the charts in monitoring shift in the process mean. The zero-state performance is obtained under the assumption that the process shift occurred during the initial stage, while the steady-state performance is study under the assumption that the process shift occurred after the process had been in control for some time. Several approaches, including integral equations, Markov chain methods and Monte Carlo simulation have been examined in statistical process control literature to obtain the run-length properties of control charts. Here, we employ the most commonly used approach based on Monte Carlo Simulation (developed in R software [27]) in our work.

A detailed evaluation of the charts in detecting shifts in the process mean is provided in terms of their average run length (ARL) and standard deviation of the run length (SDRL) performance. ARL is the average number of plotted statistics on the chart before a shift is detected [12], [13]. The in-control (IC) ARL, denoted by ARL_0, is the ARL value for an IC process. In contrast, the out-of-control (OOC) ARL, denoted by ARL_1, is the ARL value for an OOC process. SDRL is used to measure the variation of the run-length distribution for a given value of shift. Similarly, SDRL_0 and SDRL_1 are the SDRL for the IC and OOC process, respectively. When comparing two charts, the ARL_0 is fixed to a desired value. The chart with a smaller value of ARL_1 is more effective in detecting the shift in the process parameters, as compared to the other charts. We aim to recommend the choice of the one-sided or two one-sided control chart that gives the best performance. The effects of δ and the smoothing parameter w on the proposed charts are also studied.

A. ZERO-STATE RUN-LENGTH PERFORMANCE EVALUATION OF THE CHARTS

We examined the zero-state run-length performance of the charts with $w \in \{0.05, 0.10\}$, and find the corresponding value of h for each value of w that fixes ARL_0 to the desired level. We used the binary search algorithm similar to the one employed in [12], [28] to obtain the values of h that fix ARL_0 values of the charts to 200 or 370. The values of h for different combinations of w (the smoothing parameter) that fix ARL_0 of the charts are given in the last column of Tables 1 to 4. It is seen from the tables that for a fixed value of w (or p), the value of h increases with an increase in the value of p (or w, respectively).

The ARL and SDRL values of the charts are investigated under different shift, δ, sizes, and obtained from extensive simulation studies as follows:

1. At each time i, we generate individual-observation multivariate normally distributed sample with shift of size δ in the IC mean vector $\boldsymbol{\mu}_0$ and covariance matrix $\boldsymbol{\Sigma}_0 = \boldsymbol{I}_{p\times p}$, where $\delta = 0$ implies there is no shift in the process.
2. We compute the plotting statistic of the charts and compare it against the chart's limit.
3. If the chart statistic falls below the limit (in step 2), the process is declared to be IC, then repeats steps (1-2) for the monitoring of the next test sample $i+1$. Alternatively, if the test statistic falls outside the limit, the process is said to have shifted to an OOC state. Consequently, the monitoring process terminates, and we record the iteration number that gives the first OOC signal as a single run length.

We repeat the iterations 100, 000 times, and compute the ARL and SDRL as the mean and standard deviation of the 100,000 run-lengths. The zero-state ARL values of the OMHWMAI, OMHWMAII, TMHWMAI and TMHWMAII charts across simulations are reported in Tables 1 to 4, respectively. Also, the zero-state SDRL values of the charts are provided in Tables 5 to 8, respectively.

The zero-state ARL values (in Tables 1 to 4) and SDRL values (in Tables 5 to 7) can be summarized as follows:

- The ARL_1 values of charts are smaller than the corresponding ARL_0 for any choice of δ examined, which shows the charts are ARL unbiased.

TABLE 1. The zero-state ARL values of the OMHWMAI chart, the chart's parameters w and h are chosen to fix ARL_0 to 200 or 370.

ARL_0	w	p	δ											h
			0	0.05	0.1	0.2	0.5	0.75	1	1.5	2	3	5	
200	0.05	2	201.02	150.94	116.64	69.41	20.37	10.11	6.30	3.28	2.12	1.28	1.00	7.618
		3	199.70	156.30	120.38	73.37	22.87	11.41	7.27	3.47	2.34	1.35	1.00	10.027
		4	198.80	160.02	128.57	79.76	25.10	12.55	7.72	3.83	2.45	1.40	1.01	12.226
		5	200.53	165.21	130.33	83.43	26.94	14.09	8.24	4.01	2.59	1.47	1.01	14.164
		10	200.97	174.13	142.59	93.37	32.25	16.51	9.71	4.67	2.91	1.60	1.02	22.471
	0.10	2	200.57	155.92	119.64	79.02	27.89	14.70	8.77	4.38	2.70	1.47	1.01	11.965
		3	199.02	158.29	129.10	86.31	31.22	16.79	10.06	4.86	3.02	1.60	1.01	14.880
		4	200.33	163.24	132.02	89.17	33.61	18.29	11.11	5.21	3.19	1.68	1.02	17.374
		5	198.58	166.82	137.21	94.09	35.94	19.90	11.86	5.55	3.40	1.74	1.03	19.687
		10	199.54	168.16	142.74	102.08	43.11	23.36	14.25	6.68	3.90	1.98	1.04	29.011
370	0.05	2	370.78	259.46	187.79	104.99	29.79	14.45	8.43	4.06	2.62	1.44	1.01	10.708
		3	370.63	275.60	206.68	119.25	34.65	17.00	9.68	4.65	2.91	1.56	1.01	13.597
		4	370.96	283.74	212.68	126.03	37.43	18.21	10.67	4.95	3.06	1.64	1.01	15.952
		5	369.56	283.79	220.44	132.19	39.82	19.85	11.38	5.24	3.22	1.71	1.02	18.018
		10	370.88	300.63	243.65	150.48	48.79	24.15	13.90	6.36	3.76	1.92	1.05	27.160
	0.1	2	369.31	268.89	202.84	121.51	39.02	19.52	11.67	5.44	3.27	1.71	1.02	16.003
		3	369.33	279.74	213.33	133.02	43.50	22.25	13.24	6.08	3.70	1.88	1.03	19.199
		4	369.82	283.02	222.62	139.43	47.56	24.26	14.45	6.61	3.93	1.98	1.04	21.792
		5	370.58	291.19	229.54	146.95	50.50	26.25	15.60	7.12	4.12	2.09	1.05	24.339
		10	369.02	303.13	243.94	164.00	60.90	31.43	19.20	8.62	4.93	2.39	1.10	34.372

TABLE 2. The zero-state ARL values of the OMHWMAII chart, the chart's parameters w and h are chosen to fix ARL_0 to 200 or 370.

ARL_0	w	p	δ											h
			0.00	0.05	0.10	0.20	0.50	0.75	1.00	1.50	2.00	3.00	5.00	
200	0.050	2	199.08	116.04	76.87	38.83	12.09	6.88	4.66	2.80	1.98	1.24	1.00	7.253
		3	201.50	125.54	80.57	42.81	13.64	7.67	5.25	3.04	2.19	1.34	1.00	10.214
		4	200.85	125.66	83.93	47.10	14.63	8.58	5.51	3.32	2.36	1.41	1.01	12.750
		5	199.05	125.50	86.78	48.27	15.83	8.77	5.72	3.44	2.47	1.47	1.01	15.006
		10	199.51	128.28	92.58	52.25	17.45	10.06	6.83	3.89	2.75	1.64	1.02	24.409
	0.100	2	200.31	126.89	89.07	49.30	17.34	9.71	6.31	3.64	2.45	1.45	1.01	11.981
		3	199.08	134.72	94.12	55.60	18.69	10.57	7.02	3.94	2.70	1.56	1.01	15.419
		4	200.07	138.68	97.90	57.44	19.93	11.42	7.38	4.26	2.93	1.70	1.02	18.238
		5	199.84	136.45	96.89	59.24	21.09	11.80	7.84	4.42	2.96	1.76	1.03	20.692
		10	200.39	143.01	104.32	61.32	22.80	13.34	8.89	4.91	3.36	1.98	1.06	30.940
370	0.05	2	369.88	198.02	124.46	60.70	17.44	9.41	6.16	3.50	2.43	1.42	1.01	10.812
		3	370.46	204.80	130.37	66.11	19.72	10.47	6.83	3.88	2.67	1.56	1.01	14.102
		4	369.95	213.51	136.63	71.95	20.59	11.33	7.36	4.15	2.83	1.68	1.02	16.991
		5	369.76	217.03	141.45	74.76	22.05	12.02	7.67	4.37	2.99	1.75	1.03	19.452
		10	371.57	226.27	150.63	80.50	24.98	13.78	8.83	4.97	3.38	1.99	1.06	29.749
	0.1	2	370.26	212.71	139.43	72.84	22.64	12.31	7.85	4.36	2.95	1.69	1.02	16.155
		3	370.25	225.67	148.13	79.48	24.93	13.77	8.69	4.75	3.23	1.85	1.03	19.918
		4	370.95	230.45	150.66	83.42	26.51	14.45	9.25	5.13	3.42	1.96	1.04	22.905
		5	369.84	231.68	153.95	84.34	27.50	14.89	9.61	5.30	3.55	2.05	1.06	25.46
		10	369.08	235.65	160.46	89.52	30.25	16.86	10.85	5.97	3.92	2.30	1.12	36.247

- In all cases, as δ increases, the ARL_1 values approach one, which shows that the charts detect large shifts promptly.
- For a fixed value of δ, the charts are more efficient when a smaller value of w is used, which shows that a small value of w helps to detect a shift in the process mean faster.
- ARL comparison between the one-sided charts, i.e., the OMHWMA and OMHWMAII charts, show that the OMHWMAII chart (cf. Tables 2) outperforms the OMHWMAI chart (cf. Tables 1). The advantage of the OMHWMAII chart over the OMHWMAI chart is true for all values of w considered, especially for small values of δ.
- Also, ARL comparison between the two one-sided charts, i.e., the TMHWMA and TMHWMAII charts, show that the TMHWMAII chart (cf. Tables 4) outperforms the TMHWMAI chart (cf. Tables 3) for all values of w, especially for small values of δ.
- SDRL comparison of the one-sided charts, i.e., the OMHWMA and OMHWMAII charts, show the OMHWMAII chart's run-length values (cf. Tables 7) are less

TABLE 3. The zero-state ARL values of the TMHWMAI chart, the chart's parameters w and h are chosen to fix ARL_0 to 200 or 370.

ARL_0	w	p	δ											h
			0	0.05	0.1	0.2	0.5	0.75	1	1.5	2	3	5	
200	0.05	2	200.80	186.11	153.60	93.07	27.11	13.25	8.08	4.00	2.57	1.43	1.01	10.299
		3	200.00	187.53	156.08	100.22	30.07	15.24	9.00	4.40	2.79	1.55	1.01	12.876
		4	199.32	187.04	163.52	104.07	32.06	16.70	9.70	4.73	2.95	1.58	1.01	15.108
		5	200.19	189.97	164.01	109.04	34.44	17.68	10.38	4.87	3.11	1.66	1.02	17.145
		10	200.08	190.19	172.43	121.28	41.34	20.93	12.55	5.82	3.49	1.85	1.03	25.971
	0.1	2	200.20	182.61	163.66	107.86	36.05	18.63	11.03	5.21	3.22	1.68	1.01	15.273
		3	199.82	187.38	167.28	117.36	40.47	21.23	12.45	5.85	3.53	1.82	1.02	18.312
		4	200.53	195.91	171.73	122.56	44.25	22.71	13.62	6.37	3.76	1.93	1.03	20.877
		5	199.24	193.31	172.81	124.79	46.13	24.16	14.40	6.74	3.90	2.02	1.04	23.120
		10	199.68	193.46	176.71	134.84	54.99	29.33	17.57	8.24	4.63	2.29	1.08	32.859
370	0.05	2	369.90	333.84	252.09	141.98	38.66	18.62	10.78	5.05	3.09	1.64	1.01	13.833
		3	369.29	332.71	266.88	155.06	43.22	21.01	12.06	5.57	3.37	1.76	1.02	16.651
		4	370.99	341.13	280.01	166.28	46.96	23.16	13.26	6.02	3.59	1.87	1.03	19.22
		5	369.41	336.12	279.81	170.22	49.59	24.59	13.85	6.35	3.78	1.95	1.03	21.306
		10	371.69	347.26	296.86	192.43	59.98	29.57	17.18	7.57	4.42	2.21	1.07	30.775
	0.1	2	369.78	339.86	277.74	165.96	49.43	24.01	14.02	6.37	3.80	1.95	1.03	19.493
		3	369.05	345.98	286.54	179.73	54.73	27.21	16.11	7.25	4.19	2.11	1.05	22.743
		4	370.18	345.78	295.78	187.08	59.82	29.54	17.39	7.79	4.52	2.27	1.07	25.487
		5	369.99	347.30	300.04	196.93	63.19	32.11	18.68	8.37	4.74	2.35	1.08	27.896
		10	371.70	355.09	311.76	218.92	75.11	38.84	22.77	10.26	5.70	2.69	1.16	38.371

TABLE 4. The zero-state ARL values of the TMHWMAII chart, the chart's parameters w and h are chosen to fix ARL_0 to 200 or 370.

ARL_0	w	p	δ											h
			0.00	0.05	0.10	0.20	0.50	0.75	1.00	1.50	2.00	3.00	5.00	
200	0.050	2	195.38	173.27	129.68	69.87	19.81	10.48	6.99	3.86	2.66	1.54	1.01	12.742
		3	201.34	176.28	133.93	72.94	22.24	11.74	7.59	4.17	2.92	1.66	1.02	15.899
		4	198.63	179.32	134.29	76.55	22.92	12.30	8.06	4.43	3.02	1.76	1.02	18.559
		5	196.60	175.71	135.51	79.23	23.75	12.80	8.31	4.65	3.09	1.85	1.04	20.933
		10	195.25	178.65	140.04	81.92	26.79	14.77	9.35	5.16	3.52	2.06	1.07	31.059
	0.100	2	201.37	182.33	142.45	79.27	24.07	13.18	8.46	4.70	3.16	1.79	1.02	17.702
		3	192.05	174.81	142.46	84.19	25.75	14.40	9.21	4.94	3.31	1.89	1.03	20.900
		4	196.24	177.42	146.06	87.91	28.19	15.07	9.81	5.24	3.53	2.02	1.05	23.882
		5	200.17	185.14	146.72	88.78	28.74	15.69	10.14	5.49	3.66	2.11	1.07	26.515
		10	201.08	185.57	154.16	92.53	31.16	17.61	11.37	6.17	4.03	2.36	1.13	37.329
370	0.05	2	370.09	305.08	203.64	98.68	25.96	13.55	8.55	4.69	3.17	1.80	1.02	16.914
		3	370.82	314.18	209.99	105.46	28.92	14.91	9.33	5.08	3.43	1.96	1.04	20.347
		4	370.74	312.06	216.73	109.20	30.41	15.63	9.90	5.36	3.59	2.06	1.05	23.22
		5	369.03	308.69	214.47	109.87	31.65	16.51	10.34	5.54	3.71	2.14	1.07	25.653
		10	371.28	319.58	231.26	119.81	34.77	18.58	11.68	6.17	4.16	2.43	1.14	36.627
	0.1	2	370.20	315.25	222.82	108.86	30.18	15.80	10.08	5.33	3.57	2.03	1.04	21.864
		3	370.97	323.21	228.74	114.62	32.61	17.15	10.98	5.72	3.79	2.18	1.07	25.471
		4	370.43	317.64	231.47	120.60	34.14	18.23	11.60	6.05	4.00	2.32	1.08	28.454
		5	370.81	323.70	237.19	122.76	35.66	19.17	11.98	6.34	4.13	2.37	1.12	31.162
		10	370.08	327.82	241.80	129.81	39.00	21.03	13.25	7.06	4.56	2.66	1.22	42.375

variable than the run-length values of the OMHWMAI chart (cf. Tables 5) when $\delta \geq 0.10$, for all values of w. In contrast, the OMHWMAI chart gives less variable run-length results than the OMHWMAII chart when $\delta \leq 0.05$.

- Similarly, SDRL comparison of the two one-sided charts, i.e., the TMHWMA and TMHWMAII charts, show the TMHWMAII chart's run length (cf. Tables 7) are less variable than the run length of the TMHWMAI chart (cf. Tables 5) when $\delta \geq 0.10$, for all values of w (especially for small values of p). In contrast, the OMHWMAI chart gives less variable run-length results than the OMHWMAII chart when $\delta < 0.10$.
- For all values of w considered, the charts' SDRL values approach zero as the value of δ increases, demonstrating the charts' ability to detect a large shift promptly.

B. STEADY-STATE ARL PERFORMANCE OF THE CHARTS

To study the steady-state ARL performance of the charts, we adopted the scheme employed by [12], [29], by assuming that for a fixed integer s, the process is under control for the first $s-1$ samples and out-of-control after the

TABLE 5. The zero-state SDRL values of the OMHWMAI chart, the chart's parameters w and h are chosen to fix ARL_0 to 200 or 370.

charts	w	p	δ										
			0.00	0.05	0.10	0.20	0.50	0.75	1.00	1.50	2.00	3.00	5.00
200	0.05	2	171.14	128.8	97.01	60.28	18.27	8.99	5.34	2.45	1.45	0.7	0.09
		3	157.46	132.73	100.52	63.24	20.13	10.28	6.19	2.58	1.6	0.78	0.08
		4	160.28	130.13	104.83	67.72	22.44	11.3	6.54	2.86	1.71	0.83	0.09
		5	158.44	135.1	108.22	70.03	23.96	12.53	7.07	3.04	1.83	0.91	0.11
		10	158.74	136.52	114.79	77.47	27.95	14.86	8.62	3.74	2.14	1.03	0.21
	0.1	2	147.96	114.31	86.66	55.98	20.25	10.67	6.37	2.91	1.69	0.85	0.09
		3	138.51	111.07	89.47	59.74	21.46	11.79	7.02	3.15	1.9	0.95	0.14
		4	140.44	110.29	89.97	60.83	23.71	12.68	7.82	3.5	2.02	1.01	0.16
		5	137.04	113.5	91.42	63.54	24.48	13.48	8.28	3.79	2.15	1.06	0.2
		10	133.87	112.9	92.36	67.32	28.33	15.72	9.89	4.66	2.55	1.22	0.26
370	0.05	2	267.76	186.21	134.04	77.68	23.45	11.33	6.45	2.84	1.69	0.85	0.10
		3	256.84	189.97	145.64	85.28	26.02	13.05	7.44	3.28	1.89	0.97	0.13
		4	249.76	194.76	148.05	88.19	28.05	14.02	8.13	3.49	1.97	1.02	0.15
		5	247.98	190.04	150.09	90.99	29.63	15.16	8.74	3.67	2.10	1.07	0.18
		10	242.04	197.18	161.56	101.56	35.26	18.02	10.61	4.63	2.51	1.24	0.29
	0.1	2	264.91	188.89	138.88	79.63	24.38	12.56	7.62	3.37	1.88	1.00	0.15
		3	254.42	193.75	143.58	85.49	26.75	14.00	8.43	3.74	2.13	1.10	0.20
		4	249.27	191.98	146.35	87.77	28.52	15.11	9.09	4.07	2.27	1.16	0.24
		5	251.69	191.74	151.00	92.09	30.30	15.79	9.59	4.40	2.40	1.21	0.28
		10	240.01	197.07	155.10	101.48	35.05	18.33	11.63	5.26	2.94	1.39	0.40

TABLE 6. The zero-state SDRL values of the OMHWMAII chart, the chart's parameters w and h are chosen to fix ARL_0 to 200 or 370.

charts	w	p	δ										
			0.00	0.05	0.10	0.20	0.50	0.75	1.00	1.50	2.00	3.00	5.00
200	0.05	2	238.64	131.98	84.91	40.51	11.45	5.69	3.43	1.80	1.24	0.64	0.05
		3	228.79	138.64	86.26	43.71	12.71	6.49	3.90	1.99	1.38	0.75	0.08
		4	226.11	135.42	87.66	47.79	13.26	7.22	4.06	2.14	1.41	0.81	0.11
		5	216.60	132.75	90.05	48.29	14.04	7.28	4.25	2.19	1.49	0.87	0.13
		10	214.21	134.24	95.36	51.30	15.61	8.22	5.11	2.50	1.65	0.98	0.20
	0.10	2	195.29	117.02	80.02	41.61	12.91	6.96	4.25	2.15	1.37	0.80	0.09
		3	190.82	121.78	80.85	45.97	13.90	7.43	4.54	2.29	1.46	0.88	0.14
		4	195.54	124.43	85.05	47.82	14.49	8.00	4.89	2.41	1.57	0.95	0.15
		5	183.92	123.72	83.53	48.00	15.14	8.08	5.01	2.47	1.57	0.98	0.21
		10	183.00	127.34	87.18	49.63	16.47	8.98	5.74	2.80	1.75	1.08	0.29
370	0.05	2	375.08	190.86	118.10	54.44	14.43	7.05	4.20	2.08	1.43	0.82	0.09
		3	365.06	194.81	119.68	58.89	15.75	7.85	4.64	2.28	1.52	0.92	0.13
		4	364.17	201.48	123.40	61.92	16.24	8.33	5.00	2.44	1.58	0.99	0.16
		5	361.83	201.13	124.95	64.02	17.58	8.82	5.24	2.52	1.61	1.02	0.23
		10	360.83	205.03	132.29	67.85	19.50	10.08	6.00	2.91	1.82	1.13	0.33
	0.1	2	334.69	186.36	117.22	56.51	15.72	7.98	4.78	2.32	1.50	0.94	0.16
		3	347.96	198.13	123.50	61.68	16.77	8.74	5.16	2.52	1.58	1.01	0.19
		4	349.50	199.90	121.31	62.48	17.65	9.12	5.48	2.67	1.66	1.04	0.25
		5	343.20	199.85	125.77	62.94	18.29	9.32	5.75	2.77	1.71	1.08	0.29
		10	337.58	203.63	129.43	67.10	19.99	10.48	6.46	3.14	1.91	1.15	0.41

$(s+1)th$ sample. Hence, the steady-state out-of-control ARL is obtained by subtracting $s-1$ from a simulated run length. Without loss of generality, we used $s = \{10, 20, 50 \text{ or } 100\}$. Table 9 presents the steady-state ARL values of the charts when $p = 3$ or 5, $w = 0.1$ and $ARL_0 = 200$. Similar to the zero-state ARL comparison of the charts (see Tables 1 to 4 for the zero-state ARL values of the charts), steady-state ARL comparisons of the one-sided charts show that the OMHWMAII chart outperforms the OMHWHI chart. Also, the steady-state ARL comparisons of the two-sided charts show that the TMHWMAII chart outperforms the TMWH-MAI chart. The results in Table 9 show that the steady-state performance of the charts depends on the choice of s and the size of shift δ. As shown on the table, the use of a

TABLE 7. The zero-state SDRL values of the TMHWMAI chart, the chart's parameters w and h are chosen to fix ARL_0 to 200 or 370.

charts	w	p	δ										
			0.00	0.05	0.10	0.20	0.50	0.75	1.00	1.50	2.00	3.00	5.00
200	0.05	2	155.26	143.39	118.31	73.36	21.53	10.31	6.25	2.8	1.66	0.85	0.1
		3	152.22	143.7	120.48	78.30	23.81	11.66	6.96	3.06	1.81	0.95	0.12
		4	150.96	144.02	125.24	81.00	25.24	12.84	7.49	3.42	1.95	0.99	0.14
		5	151.36	144.34	123.71	84.73	26.71	13.68	8.07	3.48	2.04	1.04	0.17
		10	149.83	146.16	132.11	90.85	31.81	16.23	9.72	4.33	2.43	1.2	0.25
	0.1	2	132.68	124.34	110.88	71.56	22.96	12.07	7.23	3.28	1.84	0.98	0.13
		3	126.52	124.25	109.18	74.79	25.53	13.48	8.17	3.63	2.06	1.07	0.17
		4	130.83	127.26	110.99	79.72	27.47	14.72	8.54	4.03	2.19	1.15	0.2
		5	128.23	125.6	108.31	79.87	28.51	15.26	9.18	4.22	2.3	1.18	0.25
		10	124.98	122.68	111.6	83.47	33.67	17.9	10.85	5.19	2.77	1.37	0.37
370	0.05	2	239.75	218.61	170.55	93.87	26.46	12.97	7.55	3.22	1.87	1.00	0.14
		3	232.06	211.28	172.53	100.83	28.74	14.57	8.43	3.62	2.03	1.08	0.19
		4	234.03	215.53	177.01	105.32	30.58	15.52	9.04	3.92	2.21	1.15	0.21
		5	228.02	208.75	178.35	107.35	32.13	16.34	9.48	4.20	2.33	1.20	0.24
		10	228.78	212.63	184.36	118.88	37.74	19.04	11.62	5.12	2.81	1.37	0.35
	0.1	2	245.27	226.04	181.07	106.84	29.32	14.20	8.40	3.67	2.03	1.09	0.20
		3	239.70	225.03	187.17	112.63	32.04	15.76	9.43	4.20	2.29	1.18	0.26
		4	236.41	221.23	189.62	117.55	34.25	17.05	10.08	4.52	2.47	1.25	0.32
		5	234.67	219.84	188.48	120.39	35.56	17.84	10.70	4.85	2.61	1.28	0.34
		10	232.31	221.67	191.84	130.78	40.82	20.90	12.49	5.85	3.23	1.45	0.49

TABLE 8. The zero-state SDRL values of the TMHWMAII chart, the chart's parameters w and h are chosen to fix ARL_0 to 200 or 370.

charts	w	p	δ										
			0.00	0.05	0.10	0.20	0.50	0.75	1.00	1.50	2.00	3.00	5.00
200	0.05	2	179.56	158.59	120.97	61.29	15.39	7.51	4.63	2.18	1.50	0.91	0.13
		3	181.57	163.46	120.78	62.38	17.39	8.49	4.99	2.40	1.60	0.98	0.17
		4	181.26	163.27	121.71	64.52	17.59	8.74	5.46	2.55	1.61	1.03	0.20
		5	182.40	161.93	124.76	67.75	18.24	9.13	5.56	2.66	1.66	1.07	0.25
		10	185.19	167.86	128.85	69.36	20.34	10.64	6.29	2.90	1.83	1.14	0.35
	0.10	2	160.32	144.20	113.50	60.06	16.25	8.25	4.99	2.43	1.55	0.98	0.18
		3	158.93	142.37	114.59	64.10	16.96	8.94	5.44	2.55	1.60	1.02	0.22
		4	164.02	141.74	117.79	67.49	18.77	9.44	5.76	2.75	1.69	1.07	0.26
		5	165.90	155.45	117.61	66.90	18.55	9.46	5.95	2.87	1.76	1.08	0.31
		10	172.28	152.72	126.37	69.28	20.34	10.83	6.63	3.17	1.93	1.15	0.43
		20	165.90	155.45	117.61	66.90	18.55	9.46	5.95	2.87	1.76	1.08	0.31
370	0.05	2	296.40	251.60	164.32	75.37	18.22	8.83	5.23	2.44	1.62	1.04	0.18
		3	302.17	256.57	170.41	79.00	19.73	9.74	5.76	2.66	1.65	1.09	0.25
		4	304.92	253.65	172.94	82.72	20.64	10.12	6.05	2.80	1.73	1.13	0.28
		5	302.06	253.75	170.07	82.43	21.32	10.62	6.21	2.87	1.78	1.15	0.34
		10	310.40	262.64	184.69	87.42	23.50	11.90	7.04	3.27	2.01	1.22	0.48
	0.1	2	305.92	259.15	179.34	79.93	18.63	9.36	5.63	2.59	1.60	1.06	0.24
		3	312.44	268.21	182.96	84.34	20.08	9.92	5.98	2.81	1.68	1.08	0.32
		4	314.20	257.62	187.09	86.61	20.95	10.40	6.36	2.97	1.77	1.11	0.35
		5	310.00	269.17	190.82	89.90	21.82	10.88	6.56	3.13	1.82	1.12	0.41
		10	318.79	275.19	196.21	94.51	23.88	11.89	7.25	3.47	2.05	1.18	0.55

small value of s leads to better performance when interest lies in detecting a large shift in the process mean—however, a large value of s leads to faster detection of a large shift in the mean. Also, the charts' zero-state and steady-state ARL values show better detection ability under zero-state than the steady-state.

C. COMPARISON WITH EXISTING CHARTS

We provide the zero-state ARL comparisons of the proposed one-sided and two one-sided charts with the classical as well as the one-sided and two one-sided versions of the classical MEWMA chart [6], and MCUSUM chart [3]. The one-sided and two one-sided versions of the MCUSUM charts are

TABLE 9. The steady-state ARL values of the charts when $p = 3$ or 5, the charts' parameters w and h are chosen to fix ARL_0 to 200.

Charts	p	s	δ										
			0	0.05	0.1	0.2	0.5	0.75	1	1.5	2	3	5
OMHWMAI	3	10	197.56	158.84	130.43	88.78	37.27	22.18	15.06	8.63	5.81	3.46	2.00
		20	196.50	161.26	128.19	88.87	38.63	24.04	16.59	9.70	6.44	3.60	1.75
		50	198.82	160.76	131.96	93.48	42.56	26.62	18.55	10.52	6.65	3.27	1.29
		100	201.17	162.83	135.51	95.82	45.30	28.34	19.87	10.76	6.32	2.77	1.12
	5	10	201.63	166.97	139.23	99.54	42.48	25.73	17.40	9.96	6.72	3.95	2.23
		20	197.40	164.09	140.21	98.19	44.71	27.68	19.33	11.24	7.51	4.25	2.01
		50	197.31	163.90	140.30	100.00	47.64	30.84	21.48	12.29	7.95	3.91	1.45
		100	203.87	169.68	141.82	106.27	50.92	32.98	22.85	12.67	7.73	3.31	1.21
OMHWMAII	3	10	197.93	133.96	98.40	59.04	23.45	15.00	10.83	6.89	5.07	3.34	2.09
		20	196.13	135.19	99.37	61.21	26.06	16.73	12.29	7.79	5.66	3.54	1.94
		50	197.97	139.31	102.17	66.52	29.23	19.51	14.18	8.82	6.10	3.36	1.49
		100	200.03	140.69	105.96	69.79	32.77	21.84	15.72	9.22	6.04	2.93	1.21
	5	10	199.84	138.35	101.65	63.89	25.99	16.46	11.82	7.57	5.56	3.62	2.24
		20	196.03	137.95	103.23	65.70	28.39	18.45	13.31	8.49	6.12	3.86	2.11
		50	202.72	139.90	107.08	71.31	32.12	21.01	15.45	9.75	6.80	3.80	1.66
		100	204.42	143.92	112.01	73.60	35.15	23.50	17.15	10.26	6.80	3.44	1.32
TMHWMAI	3	10	199.64	189.03	170.57	121.71	47.95	27.95	18.38	10.31	6.90	4.02	2.24
		20	197.79	191.29	171.68	123.46	51.47	30.83	20.78	11.82	7.85	4.36	2.06
		50	201.90	196.79	175.10	130.69	56.98	35.23	24.29	13.39	8.53	4.01	1.37
		100	199.57	191.56	174.63	133.69	61.87	38.37	25.88	13.78	8.00	3.24	1.14
	5	10	200.65	193.37	175.56	133.04	54.85	31.89	21.55	12.01	8.07	4.70	2.57
		20	197.89	191.97	177.30	132.56	58.42	35.29	24.28	13.90	9.34	5.21	2.45
		50	197.04	192.79	176.95	138.06	64.31	40.64	28.22	16.11	10.39	5.00	1.62
		100	198.92	192.71	178.19	142.91	70.20	44.80	30.84	16.61	9.96	4.06	1.25
TMHWMAII	3	10	197.89	181.97	147.81	89.37	32.10	19.50	13.66	8.50	6.05	3.95	2.40
		20	195.68	180.44	146.37	91.07	34.97	21.97	15.48	9.77	6.96	4.29	2.31
		50	200.01	185.23	153.04	100.06	41.05	26.31	19.14	11.68	8.04	4.41	1.82
		100	197.32	183.17	157.03	107.77	47.64	30.70	22.18	13.08	8.37	4.11	1.42
	5	10	198.04	182.41	151.59	94.53	34.29	21.20	14.84	9.06	6.55	4.16	2.55
		20	200.11	182.74	150.17	95.77	37.58	23.46	16.86	10.47	7.53	4.69	2.51
		50	200.44	183.13	157.51	102.14	43.87	28.23	20.32	12.57	8.67	4.89	2.04
		100	198.10	186.12	160.46	109.63	50.44	33.25	23.84	14.17	9.40	4.62	1.58

TABLE 10. The zero-state ARL values of the proposed and the existing charts when $p = 2$, the charts' parameters w and h are chosen to fix ARL_0 to 200.

Type	Chart	δ											h
		0.00	0.05	0.10	0.20	0.50	0.75	1.00	1.50	2.00	3.00	5.00	
One-sided	MCUSUM	200.30	189.90	164.64	109.12	29.60	15.36	9.79	5.79	4.12	2.69	1.82	5.50
	MEWMA	200.97	193.80	161.14	99.94	28.16	15.27	10.13	6.10	4.41	2.92	1.97	8.66
	MHWMA	200.02	185.23	143.61	82.60	24.92	13.35	8.58	4.63	3.13	1.79	1.02	8.97
	OMCUSUM	199.18	155.50	120.82	75.13	25.06	13.71	8.78	4.92	3.40	2.16	1.23	6.06
	OMEWMA	199.65	151.67	116.92	71.60	24.13	13.47	8.91	5.07	3.53	2.26	1.32	9.23
	OMHWMA	200.57	155.92	119.64	79.02	27.89	14.70	8.77	4.38	2.70	1.47	**1.01**	11.97
	OMHWMAII	202.31	**126.89**	**89.07**	**49.30**	**17.34**	**9.71**	**6.31**	**3.64**	**2.45**	**1.45**	**1.01**	11.98
Two-sided	TMCUSUM	200.36	197.79	171.31	116.61	33.10	16.73	10.47	5.77	3.92	2.44	1.46	7.14
	TMEWMA	201.85	192.15	165.67	110.01	32.61	16.79	10.56	5.84	3.97	2.48	1.50	11.66
	TMHWMA	200.20	182.61	163.66	107.86	36.05	18.63	11.03	5.21	3.22	**1.68**	**1.01**	15.27
	TMHWMAII	201.37	**182.33**	**142.45**	**79.27**	**24.07**	**13.18**	**8.46**	**4.70**	**3.16**	1.79	1.02	17.70

proposed by [25]. Also, [26] proposed the one-sided and two one-sided versions of the classical MEWMA chart. In what follows, the one-sided versions of the MCUSUM and MEWMA charts are referred to as the OMCUSUM and OMEWMA charts, respectively. Also, the two one-sided versions of the MCUSUM and MEWMA charts are referred to as the TMCUSUM and TMEWMA charts, respectively. We refer the interested reader to [25], [26] for detailed information on the one-sided and two one-sided MEWMA and MCUSUM charts.

The zero-state ARL results of the proposed charts, as well as the existing charts, are provided in Tables 10 to 13, for $p \in \{2, 4, 5, \text{ or } 10\}$. The chart's parameters are chosen to fix ARL_0 of the charts to 200. As shown in the tables, comparisons among the one-sided charts show that the proposed OMHWMAII chart outperforms the competing charts for all

TABLE 11. The zero-state ARL values of the proposed and the existing charts when $p = 4$, the charts' parameters w and h are chosen to fix ARL_0 to 200.

Type	Chart	δ											h
		0.00	0.05	0.10	0.20	0.50	0.75	1.00	1.50	2.00	3.00	5.00	
One-sided	MCUSUM	199.20	189.43	165.35	108.62	33.05	18.32	12.35	7.57	5.48	3.61	2.19	8.15
	MEWMA	198.72	195.53	169.35	116.78	34.68	18.39	12.04	7.20	5.17	3.41	2.11	12.73
	MHWMA	201.73	187.74	153.45	95.47	29.97	15.95	10.25	5.47	3.63	2.09	1.05	13.11
	OMCUSUM	200.42	164.90	130.23	83.86	29.65	16.38	11.05	6.47	4.55	2.83	1.78	8.54
	OMEWMA	200.70	164.30	128.83	82.87	29.95	16.71	10.95	6.25	4.31	2.69	1.69	13.90
	OMHWMA	200.33	163.24	132.02	89.17	33.61	18.29	11.11	5.21	3.19	**1.68**	**1.02**	17.37
	OMHWMAII	200.07	**138.68**	**97.90**	**57.44**	**19.93**	**11.42**	**7.38**	**4.26**	**2.93**	1.70	**1.02**	18.24
Two-sided	TMCUSUM	201.43	190.39	169.79	118.94	36.53	19.64	12.91	7.40	5.15	3.18	1.96	9.72
	TMEWMA	199.59	190.81	175.59	126.64	40.23	20.59	12.96	7.07	4.82	2.94	1.84	16.56
	TMHWMA	203.53	195.91	171.73	122.56	44.25	22.71	13.62	6.37	3.76	**1.93**	**1.03**	20.88
	TMHWMAII	199.24	**177.42**	**146.06**	**87.91**	**28.19**	**15.07**	**9.81**	**5.24**	**3.53**	2.02	1.05	23.88

TABLE 12. The zero-state ARL values of the proposed and the existing charts when $p = 5$, the charts' parameters w and h are chosen to fix ARL_0 to 200.

Type	Chart	δ											h
		0.00	0.05	0.10	0.20	0.50	0.75	1.00	1.50	2.00	3.00	5.00	
One-sided	MCUSUM	200.82	200.51	175.77	115.93	35.66	19.79	13.64	8.43	6.17	4.05	2.52	9.46
	MEWMA	200.19	195.61	176.55	122.34	37.65	19.83	12.98	7.65	5.46	3.59	2.19	14.56
	MHWMA	201.97	186.07	157.59	96.48	31.46	17.14	10.97	5.76	3.81	2.21	1.07	14.92
	OMCUSUM	201.02	163.92	131.51	85.67	31.47	17.73	12.13	7.25	5.06	3.17	1.96	9.68
	OMEWMA	200.84	160.67	132.58	87.10	31.69	17.56	11.76	6.71	4.61	2.86	1.80	15.86
	OMHWMA	198.58	166.82	137.21	94.09	35.94	19.90	11.86	5.55	3.40	**1.74**	**1.03**	19.69
	OMHWMAII	196.84	**136.45**	**96.89**	**59.24**	**21.09**	**11.80**	**7.84**	**4.42**	**2.96**	1.76	**1.03**	20.69
Two-sided	TMCUSUM	199.55	195.02	172.11	115.90	38.62	21.17	14.26	8.13	5.72	3.52	2.10	10.93
	TMEWMA	199.07	188.65	174.38	128.66	43.07	22.13	13.80	7.50	5.12	3.12	1.93	18.60
	TMHWMA	199.24	193.31	172.81	124.79	46.13	24.16	14.40	6.74	3.90	**2.02**	**1.04**	23.12
	TMHWMAII	200.17	**185.14**	**146.72**	**88.78**	**28.74**	**15.69**	**10.14**	**5.49**	**3.66**	2.11	1.07	26.52

values of p considered. The advantage of the OMHWMAII chart over the competing charts is uniform across all values of δ, except when $\delta \geq 3$, where the OMHWMAI chart outperform the OMHWMAII chart. Also, comparisons among the two one-sided charts show that the proposed TMHWMAII chart outperforms the competing charts for all values of p considered. The advantage of the TMHWMAII chart over the competing charts is also uniform across all values of δ, except when $\delta \geq 3$, where the TMHWMAI chart also outperform the TMHWMAII chart.

IV. ROBUSTNESS TO NON-NORMALITY OF THE PROPOSED CHARTS

The proposed charts described in Section II rely on the assumption that the process variable is multivariate normally distributed. In industrial application, the normality assumptions do not always hold [30], [31]. Hence, we study the robustness of the charts to non-normality in this section. A control chart is robust to non-normal distributions if its IC run-length distribution remains stable when the normality distributional assumption is violated [32]. That is, when the ARL_0 value of the chart under a non-normal distribution is similar (or close) to the ARL_0 of the chart from a normal distribution.

Following [31]–[34], we study the sensitivity of the charts to non-normality by considering a skewed distribution (the multivariate gamma distribution) and a heavy-tailed distribution (the multivariate Student's t-distribution). The probability density function (pdf) of the multivariate gamma distribution is denoted by $G(\alpha \times \mathbf{1}_p, \beta \times \mathbf{1}_p)$, where $\alpha > 0$ and $\beta > 0$ are the shape and scale parameters, respectively. Also, the pdf of a multivariate t-distribution is denoted by $t_2(v)$, where $v > 0$ is the size of the degrees of freedom. We refer the interested reader to [31] for details on these multivariate distributions. We investigate the robustness of the charts under a large range of the shape parameter, i.e., $\alpha \in \{1, 2, 3, 4, 5, 10, 50, 100, 1000\}$; without loss of generality, we considered scale parameter, $\beta = 1$. For the t-distribution, we consider a range of degrees of freedom (v); namely, $v \in \{4, 6, 8, 10, 15, 20, 30, 40, 50, 100, 1000\}$.

The mean vector, $\boldsymbol{\mu}_{\boldsymbol{X}_i^+}$ and covariance matrix, $\boldsymbol{\Sigma}_{\boldsymbol{X}_i^+}$, of the statistic $\boldsymbol{X}_i^+ = +\max(\mathbf{0}, \boldsymbol{X}_i)$ under multivariate gamma distribution with shape (α) and scale parameter ($\beta = 1$) can be are given as:

$$\boldsymbol{\mu}_{\boldsymbol{X}_i^+} = \frac{1}{\Gamma(\alpha)} \exp^{-\alpha} \alpha^{\alpha} \times \mathbf{1}_p \tag{11}$$

and

$$\boldsymbol{\Sigma}_{\boldsymbol{X}_i^+} = \left(\frac{\exp^{-\alpha}}{(1+\alpha)\Gamma(\alpha)} K_1 - \left(\frac{1}{\Gamma(\alpha)} \exp^{-\alpha} \alpha^{\alpha} \right)^2 \right) \boldsymbol{I}_{p \times p} \tag{12}$$

respectively, where $K_1 = \left(\exp^{\alpha} \Gamma(2+\alpha, \alpha) - \alpha^{(1+\alpha)}\right)$, $\Gamma(a, s) = \int_x^{\infty} t^{a-1} e^{-t} dt$, $s > 0, a \in R$ is the upper incomplete Gamma function [35], [36]. Also, $\boldsymbol{\mu}_{\boldsymbol{X}_i^+}$ and $\boldsymbol{\Sigma}_{\boldsymbol{X}_i^+}$

TABLE 13. The zero-state ARL values of the proposed and the existing charts when $p = 10$, the charts' parameters w and h are chosen to fix ARL_0 to 200.

Type	Chart	δ											h
		0.00	0.05	0.10	0.20	0.50	0.75	1.00	1.50	2.00	3.00	5.00	
One-sided	MCUSUM	199.50	191.63	169.82	119.11	42.92	26.10	18.61	11.94	8.80	5.85	3.62	14.90
	MEWMA	199.98	195.12	183.41	138.50	48.10	24.87	15.97	9.18	6.55	4.28	2.69	22.67
	MHWMA	199.17	189.23	165.13	109.10	37.84	20.72	13.15	6.97	4.55	2.63	1.19	23.08
	OMCUSUM	200.85	173.55	144.77	99.98	39.38	24.35	17.17	10.61	7.53	4.74	2.75	15.08
	OMEWMA	199.83	170.79	139.96	97.65	38.82	21.67	14.19	8.19	5.63	3.51	2.08	24.46
	OMHWMA	199.54	168.16	142.74	102.08	43.11	23.36	14.25	6.68	3.90	**1.98**	**1.04**	29.01
	OMHWMAII	200.39	**143.01**	**104.32**	**61.32**	**22.80**	**13.34**	**8.89**	**4.91**	**3.36**	**1.98**	1.06	30.94
Two-sided	TMCUSUM	201.32	194.09	172.42	122.79	46.42	27.71	19.29	11.84	8.38	5.23	2.99	16.57
	TMEWMA	199.74	193.08	183.57	140.77	52.44	27.04	16.75	9.19	6.21	3.77	2.17	27.51
	TMHWMA	199.68	193.46	176.71	134.84	54.99	29.33	17.57	8.24	4.63	**2.29**	**1.08**	32.86
	TMHWMAII	201.08	**185.57**	**154.16**	**92.53**	**31.16**	**17.61**	**11.37**	**6.17**	**4.03**	2.36	1.13	37.33

under multivariate t-distribution with v degrees of freedom are:

$$\boldsymbol{\mu}_{\boldsymbol{X}_i^+} = \frac{\sqrt{v}}{(v-1)Beta(\frac{v}{2},\frac{1}{2})} \times \mathbf{1}_p \tag{13}$$

and

$$\boldsymbol{\Sigma}_{\boldsymbol{X}_i^+} = \left(\frac{v}{2(v-2)} - \frac{v}{(v-1)^2 Beta(\frac{v}{2},\frac{1}{2})^2}\right)\boldsymbol{I}_{p\times p} \tag{14}$$

where $Beta(a,s) = \dfrac{\Gamma(a)\Gamma(s)}{\Gamma(a+s)}$ is the beta function.

Similarly, the mean vector, $\boldsymbol{\mu}_{\boldsymbol{X}_i^-}$ and covariance matrix, $\boldsymbol{\Sigma}_{\boldsymbol{X}_i^-}$ of the statistic $\boldsymbol{X}_i^- = -\min(\mathbf{0}, \boldsymbol{X}_i)$ under multivariate gamma distribution with shape (α) and scale parameter ($\beta = 1$) are given as:

$$\boldsymbol{\mu}_{\boldsymbol{X}_i^+} = -\frac{1}{\Gamma(\alpha)}\exp^{-\alpha}\alpha^{\alpha} \times \mathbf{1}_p \tag{15}$$

and

$$\boldsymbol{\Sigma}_{\boldsymbol{X}_i^+} = \left(\frac{\exp^{-\alpha}}{(1+\alpha)\Gamma(\alpha)}K_2 - \left(\frac{1}{\Gamma(\alpha)}\exp^{-\alpha}\alpha^{\alpha}\right)^2\right)\boldsymbol{I}_{p\times p}, \tag{16}$$

respectively, where $K_2 = (\alpha^{(1+\alpha)} + \exp^{\alpha}\Gamma(2+\alpha) - \exp^{\alpha}\Gamma(2+\alpha,\alpha))$. Also, mean vector, $\boldsymbol{\mu}_{\boldsymbol{X}_i^-}$ and covariance matrix, $\boldsymbol{\Sigma}_{\boldsymbol{X}_i^-}$ under multivariate t-distribution with v degrees of freedom are:

$$\boldsymbol{\mu}_{\boldsymbol{X}_i^-} = -\frac{\sqrt{v}}{(v-1)Beta(\frac{v}{2},\frac{1}{2})} \times \mathbf{1}_p \tag{17}$$

and

$$\boldsymbol{\Sigma}_{\boldsymbol{X}_i^-} = \left(\frac{v}{2(v-2)} - \frac{v}{(v-1)^2 Beta(\frac{v}{2},\frac{1}{2})^2}\right)\boldsymbol{I}_{p\times p} \tag{18}$$

respectively. Equation (11) through equation (18) are solved in Mathematica version 12.2 package [37].

We investigate the ARL_0 performance of the proposed charts from the multivariate gamma and multivariate t-distributions when the charts' limits h under multivariate normal distributions (given in the last column of Tables 1 to 4) are used to construct the charts' limits. The ARL_0 values of the charts under multivariate t and gamma distributions when ARL_0 are fixed to 200, $w \in \{0.03, 0.05, 0.10, 0.25, 0.5, 0.75\}$, and $p = 5$ are given in Table 14 and Table 15, respectively. The ARL_0 values of the charts under the multivariate t and gamma distributions are summarized below:

- The charts' ARL_0 values depend on the choice of the process distributions. The ARL_0 values are greatly affected (i.e., deviate from their nominal values) when a skewed distribution characterizes the process (like the multivariate gamma distribution) and less affected under a heavy-tailed distribution (like the multivariate t-distribution).
- For a fixed value of the degrees of freedom, v, (in Table 14), or shape parameter, α, (in Table 15), the ARL_0 performance of the charts depends on the smoothing parameter choice. The results show that the charts are more robust to non-normality when a small value of w is used. This implies that small values of w (i.e., $w = 0.03$ and 0.05) are fairly useful when the underlying distribution is unknown or not normal.
- Comparison between the robustness of the OMHWMAI and OMHWMAII charts shows that ARL_0 values of the OMHWMAI chart are more affected and less robust to non-normality when compared to the ARL_0 values of the OMHWMAII chart, especially for small values of w and v (or α).
- Comparison between the robustness of the TMHWMAI and TMHWMAII charts shows that ARL_0 values of the TMHWMAI chart is less robust to non-normality when compared to the OMHWMAII chart under multivariate t distribution, especially for small values of w and v (or α). However, when the TMHWMAI and TMHWMAII charts are constructed under multivariate gamma distribution, our results show that the TMHWMAI chart is more robust than the TMHWMAII chart.
- The ARL_0 values of both charts increase as the shape parameter α (for the case of the gamma distribution) or size of the degrees of freedom v (for the case of the

TABLE 14. The ARL values of the charts under multivariate t-distributions when $p = 5$.

ARL_0	w	v										
		4	6	8	10	15	20	30	40	50	100	1000
OMHWMAI	0.03	132.18	141.93	152.15	162.09	172.75	177.06	190.57	188.61	194.33	204.41	202.43
	0.05	111.64	125.33	137.37	144.74	159.08	169.56	174.14	183.20	187.41	192.58	202.07
	0.10	84.70	96.84	109.70	119.23	136.53	150.74	164.78	169.97	178.26	187.52	198.97
	0.25	54.83	63.61	74.88	83.99	102.69	117.13	135.42	149.83	159.02	178.37	202.71
	0.50	42.78	50.37	59.62	68.74	85.13	101.16	121.48	132.56	143.86	167.16	197.71
	0.75	40.07	47.32	55.48	63.41	82.18	95.52	117.96	132.95	141.63	166.46	195.06
OMHWMAII	0.03	135.73	148.41	152.57	161.21	176.67	176.26	188.74	191.95	187.73	194.11	199.68
	0.05	116.22	128.07	138.81	151.00	163.00	170.11	176.81	182.23	182.53	192.89	198.21
	0.10	87.03	100.86	111.72	123.01	140.17	152.34	162.93	173.10	176.50	185.47	197.33
	0.25	54.70	64.99	74.49	83.00	104.19	117.95	135.18	148.82	156.56	177.58	199.43
	0.50	42.58	51.25	58.67	68.49	84.98	100.40	118.01	131.15	141.10	165.25	191.92
	0.75	40.91	47.34	56.71	63.90	82.12	95.50	119.05	131.71	139.03	165.86	191.23
TMHWMAI	0.03	113.12	124.20	136.68	144.48	161.36	166.66	177.13	183.69	185.09	192.51	192.62
	0.05	94.31	107.12	119.34	130.40	148.44	157.73	171.22	177.33	181.25	193.23	200.38
	0.10	68.01	81.18	92.53	103.16	122.73	135.41	151.99	161.71	167.95	182.92	198.42
	0.25	41.34	48.37	57.73	66.14	84.10	98.35	116.99	129.58	141.47	166.01	196.24
	0.50	30.42	36.73	44.53	51.10	67.82	81.05	101.26	119.30	130.33	160.92	198.89
	0.75	27.70	33.12	40.02	46.61	61.76	77.18	99.18	112.93	123.39	156.15	194.42
TMHWMAII	0.03	125.61	136.27	145.42	153.31	169.63	175.18	180.78	188.27	186.98	195.54	199.59
	0.05	102.52	117.00	131.19	138.27	153.03	161.89	170.92	177.42	183.73	191.51	195.38
	0.10	72.15	85.74	95.64	106.59	123.64	136.97	153.38	161.30	166.91	184.65	197.98
	0.25	40.77	48.47	57.75	64.70	83.08	96.00	117.89	128.66	142.77	164.98	198.76
	0.50	29.47	35.23	42.88	49.67	67.01	78.93	99.82	114.47	124.57	153.89	195.02
	0.75	27.97	33.43	40.24	47.07	63.88	77.38	98.25	114.70	125.67	160.22	198.04

TABLE 15. The ARL values of the charts under multivariate gamma distributions when $p = 5$.

Charts	w	α								
		1	2	3	4	5	10	50	100	1000
OMHWMAI	0.03	126.79	138.61	144.02	151.90	155.68	165.72	183.05	190.25	198.49
	0.05	107.69	119.59	129.42	135.31	137.62	154.19	173.14	181.85	194.42
	0.10	82.24	94.56	102.13	108.69	113.45	129.89	156.92	169.13	187.59
	0.25	49.96	61.07	67.79	73.80	78.51	94.50	131.26	146.55	179.14
	0.50	37.45	46.41	52.83	58.17	62.51	77.17	117.23	136.57	171.70
	0.75	34.35	42.56	48.39	53.78	57.19	72.52	113.45	133.34	169.67
OMHWMAII	0.03	182.71	190.69	194.27	195.74	197.69	203.15	197.58	198.24	199.70
	0.05	140.23	154.73	162.95	165.54	167.46	176.98	190.62	193.51	199.24
	0.10	96.62	110.60	118.72	124.13	128.58	140.85	166.99	173.16	194.65
	0.25	53.81	66.11	73.38	77.68	81.51	97.18	132.96	149.78	176.88
	0.50	37.77	47.24	53.51	57.90	63.29	77.62	114.38	131.59	171.50
	0.75	34.25	42.75	48.40	53.07	58.40	72.13	111.37	128.04	170.48
TMHWMAI	0.03	158.69	170.87	178.71	180.66	184.00	191.49	196.31	198.04	196.16
	0.05	138.12	153.90	165.26	174.00	177.18	184.90	198.19	195.69	200.70
	0.10	103.75	121.58	134.58	144.79	149.49	166.65	191.12	194.13	198.67
	0.25	63.18	78.64	90.25	99.16	107.74	132.86	180.44	191.88	200.32
	0.50	47.90	62.43	73.43	83.39	88.37	115.35	172.64	185.49	201.96
	0.75	44.17	57.78	67.77	76.46	83.57	111.50	170.68	184.79	194.12
TMHWMAII	0.03	27.55	52.20	70.12	85.42	97.97	132.00	184.64	189.35	199.83
	0.05	25.11	45.78	62.67	75.91	84.43	119.28	176.23	186.39	195.20
	0.10	19.51	33.29	43.71	52.91	60.46	87.89	154.59	173.02	195.96
	0.25	10.37	16.98	21.39	25.96	29.67	46.42	106.87	139.38	194.23
	0.50	6.41	9.93	13.05	16.01	18.57	30.69	85.26	116.73	179.24
	0.75	5.28	8.07	10.98	13.90	16.38	27.29	82.23	114.28	186.77

t-distribution) increases. Hence, the ARL_0 values of the charts tend to converge to the desired nominal ARL_0 value of the chart based on the normal distribution, when a large value of v or α is used.

V. ESTIMATION OF PARAMETERS

The proposed charts described in Section II were formulated assuming that the process parameters $\boldsymbol{\mu}$ and $\boldsymbol{\Sigma}$ are both known. It may be possible that the underlying process parameters are not known and need to be estimated in practice. In such cases, the charts' implementations are in two phases (Phase I and Phase II). In Phase I, a large in-control historical sample is analysed to establish the in-control state, estimate the process parameters and the chart's limits.

The unknown process parameter $\boldsymbol{\mu}$ may be estimated using the unbiased estimator from m Phase I samples given as $\bar{\boldsymbol{Y}} = \frac{\sum_{i=1}^{m} \boldsymbol{Y}}{m}$. Some other approaches for estimating $\boldsymbol{\mu}$ have been proposed in practice. For example, [38] showed that the usual estimate $\bar{\boldsymbol{Y}}$ under sum of squares of the errors is only admissible for $p \leq 2$, but inadmissible if $p \geq 3$. He showed that there exist an estimator $\beta(Y_1, \ldots, Y_p)$, such that $L(\beta(Y_1, \ldots, Y_p), \boldsymbol{\mu_0}) \leq L(\bar{\boldsymbol{Y}}, \boldsymbol{\mu_0})$. Strict inequality holds for some $\boldsymbol{\mu_0}$ when $p \geq 3$, where $L(\beta(.), \boldsymbol{\mu_0})$ is the sum of squares of the errors of $\beta(.)$ from $\boldsymbol{\mu_0}$ given as $E((\beta(.) - \boldsymbol{\mu_0})'\boldsymbol{\Sigma_0}^{-1}(\beta(.) - \boldsymbol{\mu_0}))$. Hence, he proposed a shrinkage estimator, $\beta(Y_1, \ldots, Y_p)$, of the mean vector, that has smaller sum of squares of the errors than the usual estimator. Specifically, [38] showed that

$$\beta^{JS} = \left(1 - \frac{p-2}{m\bar{\boldsymbol{Y}}'\bar{\boldsymbol{Y}}}\right)\bar{\boldsymbol{Y}}$$

dominates $\bar{\boldsymbol{Y}}$ for any $p \geq 3$ under the assumption that $\boldsymbol{\Sigma_0} = \boldsymbol{I}_p$, where $\boldsymbol{I}$ is the $p \times p$ identity matrix. [39] gave an alternative form of the James-stein estimator for the case $\boldsymbol{\Sigma_0} = \sigma^2 \boldsymbol{I}_p$, where σ^2 is a common variance of the p random variables. The proposed estimate of $\boldsymbol{\mu}$ by [39] is given by

$$\beta^{JS1} = \left(1 - \frac{p-2}{(m\bar{\boldsymbol{Y}}'\bar{\boldsymbol{Y}})/\sigma^2}\right)\bar{\boldsymbol{Y}}.$$

More generally, when $\boldsymbol{\Sigma_0}$ is non-diagonal, the James-stein estimator has a form [40], [41]

$$\beta^{JS2} = \left(1 - \frac{p-2}{m\bar{\boldsymbol{Y}}'\boldsymbol{\Sigma_0}^{-1}\bar{\boldsymbol{Y}}}\right)\bar{\boldsymbol{Y}}.$$

Since the work of [38], several James-stein estimators have been proposed in Literature, for example, an improved estimator given as:

$$\beta^{JSI} = \left(1 - \frac{p-2}{m\bar{\boldsymbol{Y}}'\boldsymbol{\Sigma_0}^{-1}\bar{\boldsymbol{Y}}}\right)^{+}\bar{\boldsymbol{Y}},$$

where

$$y^{+} = \begin{cases} y & \text{if } y > 0 \\ 0 & \text{otherwise} \end{cases}$$

was used by [42]. Also, to overcome the singularity problem, [43] considered a special situation where $\boldsymbol{\Sigma_0}$ is diagonal, and constructed a hierarchical Bayesian model. They proposed estimator of the following form

$$\beta^{T} = \left(1 - \frac{(p-2)(p-1)}{m(m-3)\bar{\boldsymbol{Y}}'\boldsymbol{K}_m^{-1}\bar{\boldsymbol{Y}}}\right)\bar{\boldsymbol{Y}},$$

where $\boldsymbol{K}_m = Diag(\boldsymbol{\Sigma_0})$.

For the case of estimating the covariance matrix, $\boldsymbol{\Sigma}$, of individual-observations, one typical approach is to estimate it using the unbiased estimate, given as $\boldsymbol{S} = \frac{1}{m-1}\sum_{i=1}^{m}(\boldsymbol{y}_i - \bar{\boldsymbol{y}})(\boldsymbol{y}_i - \bar{\boldsymbol{y}})'$ [2]. Also, the use of mean square successive difference (MSSD) approach for estimating the variance-covariance matrix, given by $\hat{\boldsymbol{\Sigma}}_{MSSD} = \frac{\boldsymbol{V}'\boldsymbol{V}}{2(m-1)}$, where $\boldsymbol{v}_i = \boldsymbol{y}_{i+1} - \boldsymbol{y}_i$, $i = 1, 2, \ldots, m-1$, and V is a column vector, given by $\boldsymbol{V} = (\boldsymbol{v}_1^T, \boldsymbol{v}_2^T, \cdots, \boldsymbol{v}_{(m-1)}^T)'$ was proposed by [44]. [45] proposed estimator of the form $\hat{\boldsymbol{\Sigma}}_{SW} = \frac{\sum_{j=1}^{m}\boldsymbol{F}_j}{m-1}$, where $\boldsymbol{F}_i = \boldsymbol{F}_{i-1} + (y_i - \bar{y})(y_i - \bar{y})'$ where, $F_0 = 0$, $i = 1, 2, \ldots, m$. Also, use of shrinkage estimates of covariance matrix have been examined in SPC literature. For example, [12], [13] investigated the use of weighted average of the empirical unbiased estimate $\boldsymbol{S}$ and a target matrix $\boldsymbol{T}$, given as $\hat{\boldsymbol{\Sigma}}_S = \lambda\boldsymbol{T} + (1-\lambda)\boldsymbol{S}$, where $\lambda \in [0, 1]$ represents the shrinkage parameter, $\lambda = 1$ gives $\hat{\boldsymbol{\Sigma}}_S = \boldsymbol{T}$, and $\lambda = 0$ implies $\hat{\boldsymbol{\Sigma}}_S = \boldsymbol{S}$. The optimal value of λ was obtained by minimizing $R(\lambda) = ||\hat{\boldsymbol{\Sigma}}_S - \boldsymbol{\Sigma}_0||_F^2$, where, $||.||_F^2$ is the squared Frobenius norm. Some other approaches for estimating the covariance matrix include, the use of adaptive thresholding [46], penalized likelihood estimation [47]–[49], or ridge penalized likelihood ratio [50], [51].

Once $\boldsymbol{\mu}$ and $\boldsymbol{\Sigma}$ are estimated, the proposed charts can be constructed for monitoring shifts in the process mean vector in Phase II, where the process monitoring is initiated. The estimated parameters, along with the specified smoothing parameter w and the charts' limits (h), are used. At each time i in Phase II where the process might have shifted from $\boldsymbol{\mu}_0$ to $\boldsymbol{\mu}_1$, draw a random sample from the process. Compute the charts' statistics and compare them against their corresponding limits. For any of the proposed charts, if the chart's statistic is plotted above its limit, the process at time i is reported to be OOC; otherwise, the process is considered to be IC.

VI. ILLUSTRATIVE EXAMPLE

We illustrate the performance of the proposed charts using the Kulpa data set reported by Santoz-Fernandez [52]. The data set consists of $p = 2$ and $m = 113$ observations. Since the true mean vector and covariance parameters of the data are unknown. Here, we estimate them using $\bar{\boldsymbol{Y}}$ (the unbiased sample mean vector) and $\bar{\boldsymbol{S}}$ (the unbiased sample covariance matrix), respectively. The unbiased estimates $\bar{\boldsymbol{Y}}$ and $\bar{\boldsymbol{S}}$ are given as:

$$\bar{\boldsymbol{Y}} = \begin{bmatrix} 0.04452212 & 2.40780531 \end{bmatrix}$$

and

$$\boldsymbol{S} = \begin{bmatrix} 0.36733143 & 0.02028655 \\ 0.02028655 & 0.53718052, \end{bmatrix}$$

respectively.

To investigate the detection ability of the charts in Phase II, a shift of size $\delta = 0.1$ unit is added to the $m = 113$ observations. The results of the classical charts: MCUSUM,

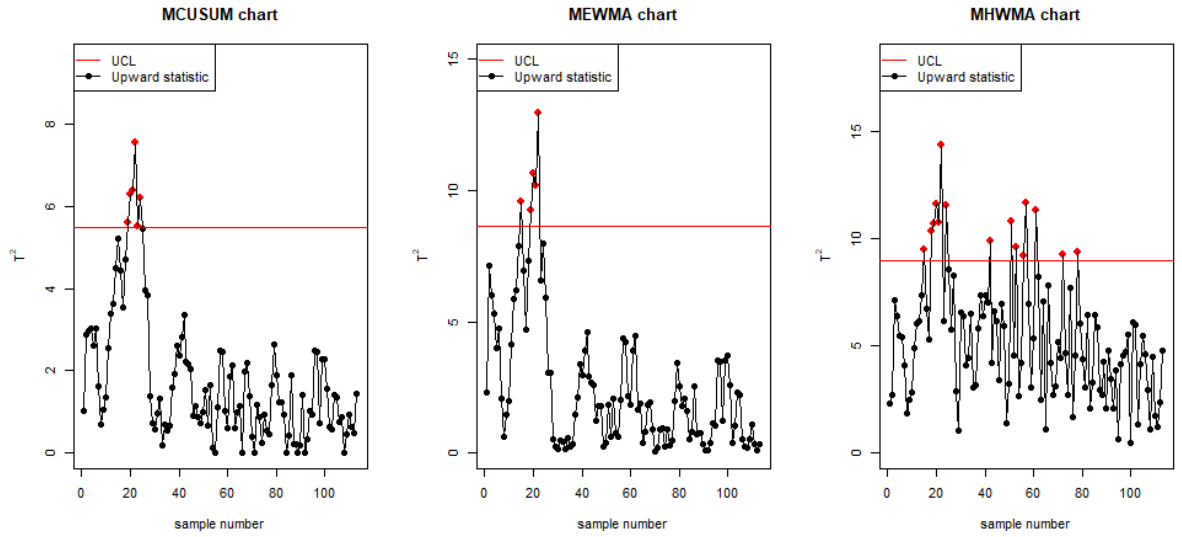

FIGURE 1. Results of the classical charts.

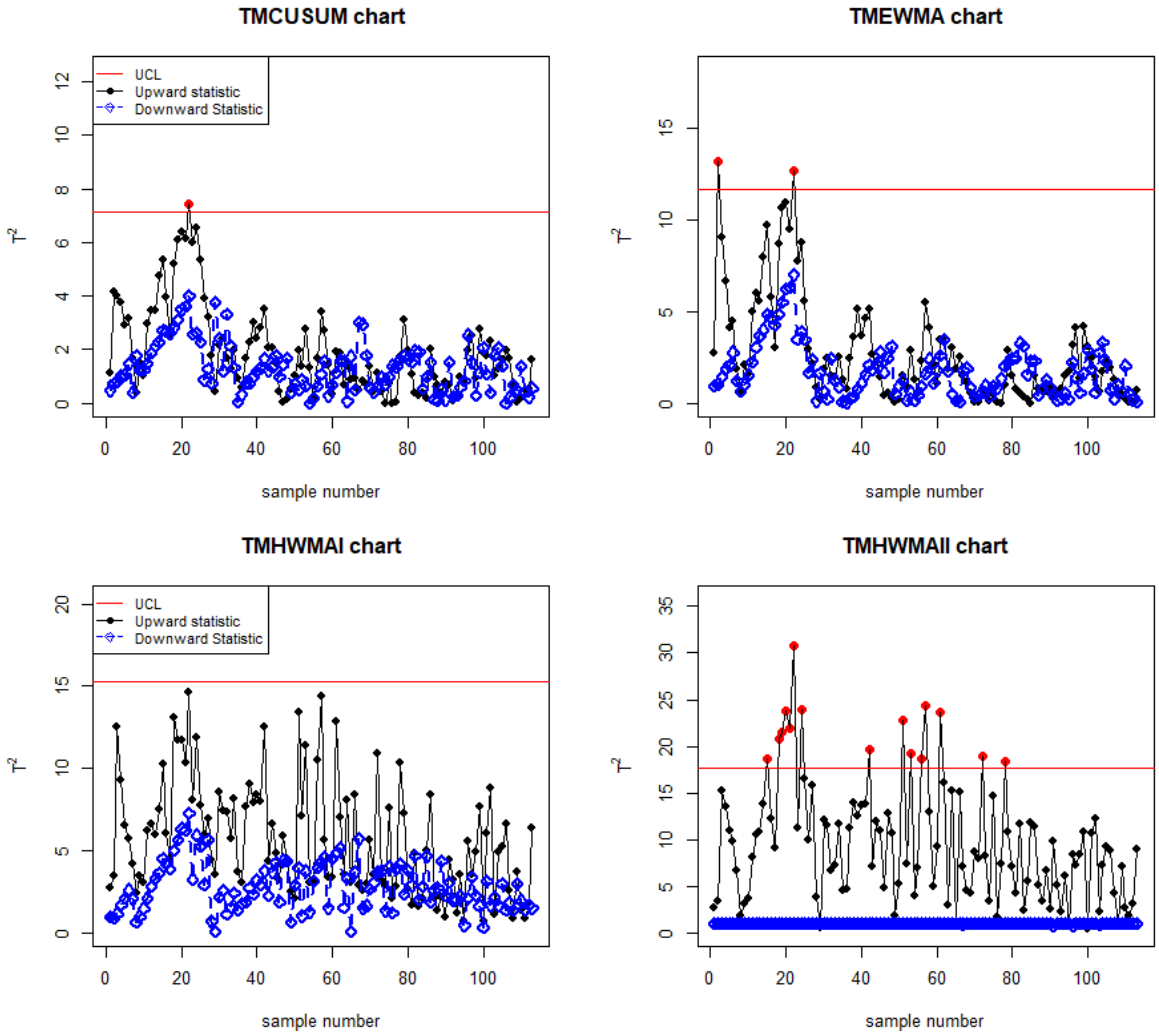

FIGURE 2. Results of the two one-sided charts.

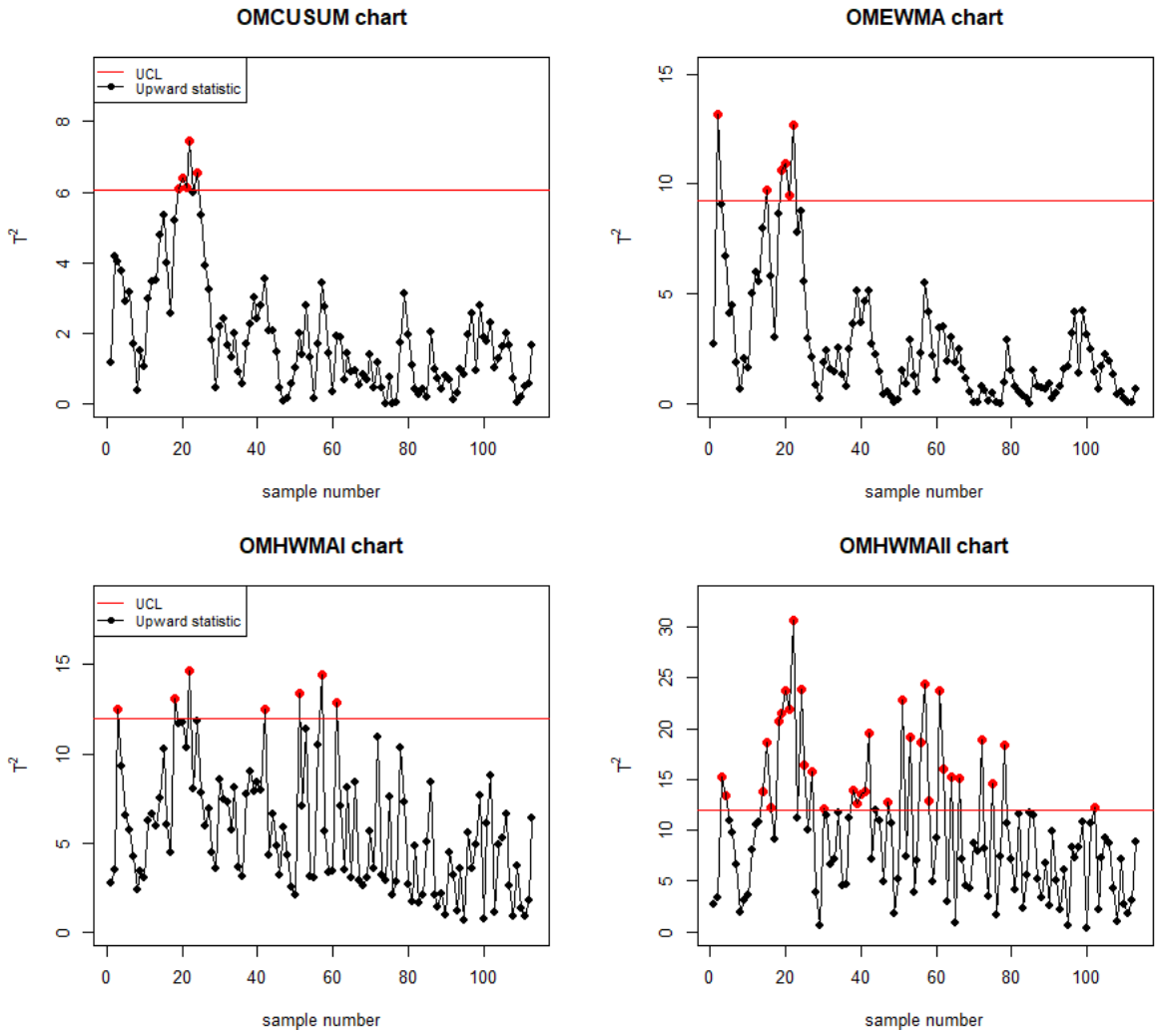

FIGURE 3. Results of the one-sided charts.

MEWMA and MHWMA charts are given in Figure 1. The results of the two-sided charts, including the TMCUSUM, TMEWMA, TMHWMAI and TMHWMAII charts, are provided in Figure 2. Also, the results of the one-sided charts, including the OMCUSUM, OMEWMA, OMHWMAI and OMHWMAII charts, are provided in Figure 3. The values of h given in Table 10 are used to fixed the in-control ARL of the charts to 200.

As shown in Figure 1, the MCUSUM, MEWMA and MHWMA charts detect six, five and fifteen out-of-control samples. In the case of monitoring both upward and downward shifts, the TMCUSUM, TMEWMA, TMHWMAI and TMHWMAII charts (in Figure 2) trigger one, two, zero, and fifteen out-of-control samples, respectively. Lastly, the OMCUSUM, OMEWMA, OMHWMAI and OMHWMAII charts used for monitoring upward shifts (in Figure 3) trigger five, six, seven, and thirty-three out-of-control samples, respectively. The results in Figures 1 to 3 demonstrate the advantage of the OMHWMAII chart (in Figure 3) over the classical MHWMA chart. The results show that using the directional sensitive OMHWMAII chart detects the shifts faster than the classical MHWMA directional invariant chart. The results also show the advantage of one-sided charts over the two one-sided charts. Finally, the results show the advantage of the OMHWMAII chart (or the TMHWMAII chart) over the competing charts when interest lies in monitoring upward shift (or both upward and downward shift, respectively) in the process mean vector.

VII. CONCLUSION

We proposed new one-sided and two one-sided control charts for monitoring shifts in the process mean vector. The proposed charts are obtained in the forms of the multivariate homogeneously weighted moving average approach that yield an efficient way to detect small shifts in the process mean. We provided simulation results under different shift sizes in the process mean vector and evaluated the performance of the proposed charts in terms of their run length

properties. Our simulation results showed that the proposed OMHWMAII chart for the case monitoring upward shifts (or proposed two one-sided TMHWMAII chart) detects smaller shifts in the mean vector more rapidly than the larger shift. In contrast, the proposed OMHWMAI chart, for the case of monitoring upward shifts (or proposed two one-sided TMHWMAI chart), detects larger shifts in the mean vector more rapidly than smaller shifts.

The average run length (ARL) comparisons of the proposed charts with the classical, one-sided and two one-sided charts versions of the MEWMA and MCUSUM charts showed that the proposed OMHWMAII chart (or TMHWMAII chart) is more efficient than the existing charts used for the same purpose, especially when interest lies in detecting a small shift in the process mean. In contrast, the proposed OMHWMAI chart (or TMHWMAI chart) outperformed the existing charts when interest lies in detecting a large shift in the process mean vector.

We investigated the charts' sensitivity to non-normal distributions and showed how they could be designed to be robust to non-normality. Simulation results showed that the proposed charts are particularly robust to non-normality when a smaller value of w is used. In particular, the charts can be designed to have IC run-length performance that is very close to that of the chart based on normal distribution when a small smoothing parameter is used. We gave a step-by-step implementation of the proposed charts when their parameters are unknown and need to be estimated from historical in-control samples. We consider that more research work on the effects of parameters estimation on the performance of the charts (in Phase II) is required in the future. Also, optimal parameters of the charts warrant study.

REFERENCES

[1] H. Hotteling, "Multivariate quality control, illustrated by the air testing of sample bombsights," *Techn. Stat. Anal.*, pp. 111–184, 1947.

[2] D. C. Montgomery, *Introduction to Statistical Quality Control*. Hoboken, NJ, USA: Wiley, 2007.

[3] R. B. Crosier, "Multivariate generalizations of cumulative sum quality-control schemes," *Technometrics*, vol. 30, no. 3, pp. 291–303, Aug. 1988.

[4] J. J. Pignatielloand, Jr., and G. C. Runger, "Comparisons of multivariate CUSUM charts," *J. Qual. Technol.*, vol. 22, pp. 173–186, Jul. 1990.

[5] E. S. Page, "Cumulative sum charts," *Technometrics*, vol. 3, no. 1, pp. 1–9, Feb. 1961.

[6] C. A. Lowry, W. H. Woodall, C. W. Champ, and S. E. Rigdon, "A multivariate exponentially weighted moving average control chart," *Technometrics*, vol. 34, no. 1, pp. 46–53, 1992.

[7] S. W. Roberts, "Control chart tests based on geometric moving averages," *Technometrics*, vol. 42, no. 1, pp. 97–101, Feb. 2000.

[8] N. A. Adegoke, S. A. Abbasi, A. N. H. Smith, M. J. Anderson, and M. D. M. Pawley, "A multivariate homogeneously weighted moving average control chart," *IEEE Access*, vol. 7, pp. 9586–9597, 2019.

[9] N. Abbas, "Homogeneously weighted moving average control chart with an application in substrate manufacturing process," *Comput. Ind. Eng.*, vol. 120, pp. 460–470, Jun. 2018.

[10] M. H. Lee and M. B. C. Khoo, "Optimal statistical designs of a multivariate CUSUM chart based on ARL AND MRL," *Int. J. Rel., Qual. Saf. Eng.*, vol. 13, no. 5, pp. 479–497, Oct. 2006.

[11] M. H. Lee, M. B. C. Khoo, and M. Xie, "An optimal control procedure based on multivariate synthetic cumulative sum," *Qual. Rel. Eng. Int.*, vol. 30, no. 7, pp. 1049–1058, Nov. 2014.

[12] N. A. Adegoke, A. N. H. Smith, M. J. Anderson, S. A. Abbasi, and M. D. M. Pawley, "Shrinkage estimates of covariance matrices to improve the performance of multivariate cumulative sum control charts," *Comput. Ind. Eng.*, vol. 117, pp. 207–216, Mar. 2018.

[13] N. A. Adegoke, A. N. H. Smith, M. J. Anderson, and M. D. M. Pawley, "MEWMA charts when parameters are estimated with applications in gene expression and bimetal thermostat monitoring," *J. Stat. Comput. Simul.*, vol. 91, no. 1, pp. 37–57, Jan. 2021.

[14] N. Abbas, M. Riaz, S. Ahmad, M. Abid, and B. Zaman, "On the efficient monitoring of multivariate processes with unknown parameters," *Mathematics*, vol. 8, no. 5, p. 823, May 2020.

[15] A. Haq, "Weighted adaptive multivariate CUSUM control charts," *Qual. Rel. Eng. Int.*, vol. 34, no. 5, pp. 939–952, Jul. 2018.

[16] A. Haq, "Weighted adaptive multivariate CUSUM charts with variable sampling intervals," *J. Stat. Comput. Simul.*, vol. 89, no. 3, pp. 478–491, Feb. 2019.

[17] A. Haq, M. B. C. Khoo, M. H. Lee, and S. A. Abbasi, "Enhanced adaptive multivariate EWMA and CUSUM charts for process mean," *J. Stat. Comput. Simul.*, pp. 1–22, Mar. 2021.

[18] S. Sukparungsee, S. Sasiwannapong, P. Busababodhin, and Y. Areepong, "The effects of constructed bivariate copulas on multivariate control charts effectiveness," *Qual. Rel. Eng. Int.*, pp. 1–13, Feb. 2021.

[19] B. Zaman, M. H. Lee, M. Riaz, and M. R. Abujiya, "An improved process monitoring by mixed multivariate memory control charts: An application in wind turbine field," *Comput. Ind. Eng.*, vol. 142, Apr. 2020, Art. no. 106343.

[20] W. Zhao, Z. Wang, and C. Wu, "Adaptive multivariate EWMA charts for monitoring sparse mean shifts based on parameter optimization design," *J. Stat. Comput. Simul.*, pp. 1–14, Mar. 2021.

[21] A. B. A. Dawod, N. A. Adegoke, and S. A. Abbasi, "Efficient linear profile schemes for monitoring bivariate correlated processes with applications in the pharmaceutical industry," *Chemometric Intell. Lab. Syst.*, vol. 206, Nov. 2020, Art. no. 104137.

[22] M. Ramos, J. Ascencio, M. V. Hinojosa, F. Vera, O. Ruiz, M. I. Jimenez-Feijoó, and P. Galindo, "Multivariate statistical process control methods for batch production: A review focused on applications," *Prod. Manuf. Res.*, vol. 9, no. 1, pp. 33–55, Jan. 2021.

[23] M. D. Joner, W. H. Woodall, M. R. Reynolds, and R. D. Fricker, "A one-sided MEWMA chart for health surveillance," *Qual. Rel. Eng. Int.*, vol. 24, no. 5, pp. 503–518, Aug. 2008.

[24] R. D. Fricker, "Directionally sensitive multivariate statistical process control methods with application to syndromic surveillance," *Adv. Disease Surv.*, vol. 3, no. 1, pp. 1–17, 2007.

[25] A. Haq and K. Sohrab, "Directionally sensitive MCUSUM mean charts," *Qual. Rel. Eng. Int.*, Feb. 2021.

[26] A. Haq, "One-sided and two one-sided MEWMA charts for monitoring process mean," *J. Stat. Comput. Simul.*, vol. 90, no. 4, pp. 699–718, Mar. 2020.

[27] R Core Team, R Foundation for Statistical Computing, Vienna, Austria. (2019). *R: A Language and Environment for Statistical Computing*. [Online]. Available: https://www.R-project.org/

[28] C. W. Champ, L. A. Jones-Farmer, and S. E. Rigdon, "Properties of the T^2 control chart when parameters are estimated," *Technometrics*, vol. 47, no. 4, pp. 437–445, 2005.

[29] H.-M. Ngai and J. Zhang, "Multivariate cumulative sum control charts based on projection pursuit," *Stat. Sinica*, 747–766, Jul. 2001.

[30] N. A. Adegoke, A. N. H. Smith, M. J. Anderson, R. A. Sanusi, and M. D. M. Pawley, "Efficient homogeneously weighted moving average chart for monitoring process mean using an auxiliary variable," *IEEE Access*, vol. 7, pp. 94021–94032, 2019.

[31] Z. G. Stoumbos and J. H. Sullivan, "Robustness to non-normality of the multivariate EWMA control chart," *J. Qual. Technol.*, vol. 34, no. 3, pp. 260–276, Jul. 2002.

[32] S. W. Human, P. Kritzinger, and S. Chakraborti, "Robustness of the EWMA control chart for individual observations," *J. Appl. Statist.*, vol. 38, no. 10, pp. 2071–2087, Oct. 2011.

[33] C. M. Borror, D. C. Montgomery, and G. C. Runger, "Robustness of the EWMA control chart to non-normality," *J. Qual. Technol.*, vol. 31, no. 3, pp. 309–316, Jul. 1999.

[34] M. Aslam, R. A. R. Bantan, and N. Khan, "Design of a control chart for gamma distributed variables under the indeterminate environment," *IEEE Access*, vol. 7, pp. 8858–8864, 2019.

[35] A. Aygüneş, "A note on polylogarithms and incomplete gamma function," *Applicable Anal. Discrete Math.*, vol. 14, no. 3, pp. 697–709, 2020.

[36] I. Pinelis, "Monotonicity properties of the gamma family of distributions," *Statist. Probab. Lett.*, vol. 171, Apr. 2021, Art. no. 109027.
[37] Wolfram Research. *Mathematica, Version 12.2*. [Online]. Available: https://www.wolfram.com/mathematica
[38] C. Stein, "Inadmissibility of the usual estimator for the mean of a multivariate normal distribution," in *Contribution to the Theory of Statistics*. Berkeley, CA, USA: Univ. California Press, 2020, pp. 197–206.
[39] A. J. Baranchik, "A family of minimax estimators of the mean of a multivariate normal distribution," *Ann. Math. Statist.*, vol. 41, no. 2, pp. 642–645, Apr. 1970.
[40] L. J. Gleser, "Minimax estimators of a normal mean vector for arbitrary quadratic loss and unknown covariance matrix," *Ann. Statist.*, vol. 14, no. 4, pp. 1625–1633, Dec. 1986.
[41] P.-E. Lin and H.-L. Tsai, "Generalized Bayes minimax estimators of the multivariate normal mean with unknown covariance matrix," *Ann. Statist.*, vol. 1, no. 1, pp. 142–145, Jan. 1973.
[42] H. Wang, L. Huwang, and J. H. Yu, "Multivariate control charts based on the James–Stein estimator," *Eur. J. Oper. Res.*, vol. 246, no. 1, pp. 119–127, Oct. 2015.
[43] T. Tong, L. Chen, and H. Zhao, "Improved mean estimation and its application to diagonal discriminant analysis," *Bioinformatics*, vol. 28, no. 4, pp. 531–537, Feb. 2012.
[44] D. S. Holmes and A. E. Mergen, "Improving the performance of the T^2 control chart," *Qual. Eng.*, vol. 5, no. 4, pp. 619–625, 1993.
[45] J. H. Sullivan and W. H. Woodall, "A comparison of multivariate control charts for individual observations," *J. Qual. Technol.*, vol. 28, no. 4, pp. 398–408, Oct. 1996.
[46] G. M. Abdella, J. Kim, S. Kim, K. N. Al-Khalifa, M. K. Jeong, A. M. Hamouda, and E. A. Elsayed, "An adaptive thresholding-based process variability monitoring," *J. Qual. Technol.*, vol. 51, no. 3, pp. 242–256, Jul. 2019.
[47] E. M. Maboudou-Tchao and V. Agboto, "Monitoring the covariance matrix with fewer observations than variables," *Comput. Statist. Data Anal.*, vol. 64, pp. 99–112, Aug. 2013.
[48] Z. Li and F. Tsung, "A control scheme for monitoring process covariance matrices with more variables than observations," *Qual. Rel. Eng. Int.*, vol. 35, no. 1, pp. 351–367, Feb. 2019.
[49] B. Li, K. Wang, and A. B. Yeh, "Monitoring the covariance matrix via penalized likelihood estimation," *IIE Trans.*, vol. 45, no. 2, pp. 132–146, Feb. 2013.
[50] J. Kim, G. M. Abdella, S. Kim, K. N. Al-Khalifa, and A. M. Hamouda, "Control charts for variability monitoring in high-dimensional processes," *Comput. Ind. Eng.*, vol. 130, pp. 309–316, Apr. 2019.
[51] W. N. van Wieringen and C. F. W. Peeters, "Ridge estimation of inverse covariance matrices from high-dimensional data," *Comput. Statist. Data Anal.*, vol. 103, pp. 284–303, Nov. 2016.
[52] E. Santos-Fernández, *Multivariate Statistical Quality Control Using R*, vol. 14. New York, NY, USA: Springer, 2012.

NURUDEEN A. ADEGOKE received the Ph.D. degree in statistics from Massey University, Auckland, New Zealand. His current research interests include statistical process control, reliability, regularization procedures, and machine learning techniques.

MUHAMMAD RIAZ is currently a Professor of statistics with the Department of Mathematics and Statistics, King Fahd University of Petroleum and Minerals, Dhahran, Saudi Arabia. His current research interests include statistical process control, nonparametric techniques, mathematical statistics, and experimental design.

KHADIJAT OLADAYO GANIYU received the bachelor's degree in food science and technology from the Federal University of Technology Akure, Nigeria. She is currently pursuing the degree in food science and technology with the University of New South Wales, Australia. She worked as a Laboratory Technician with the AsureQuality Laboratory at Auckland, Auckland, New Zealand, at the time of conducting this research work.

SADDAM AKBER ABBASI received the Ph.D. degree in statistics from The University of Auckland, New Zealand, in 2013. Before joining Qatar University, he was an Assistant Professor with the King Fahd University of Petroleum and Minerals, Dhahran, Saudi Arabia, for three years. He is currently working as an Assistant Professor with the Department of Mathematics, Statistics and Physics, Qatar University, Doha, Qatar. His research interests include SPC, time series analysis, profile monitoring, and non-parametric statistics.